European Journal of Medicinal Chemistry 257 (2023) 115515

Contents lists available at ScienceDirect

European Journal of Medicinal Chemistry

journal homepage: www.elsevier.com/locate/ejmech

Research paper

Multi-action platinum(IV) prodrugs conjugated with COX-inhibiting NSAIDs☆

Xiao Liu [a], Dominik Wenisch [b], Philipp Dahlke [c], Paul M. Jordan [c], Michael A. Jakupec [b,d], Christian R. Kowol [b,d], Phil Liebing [a], Oliver Werz [c,**], Bernhard K. Keppler [b,d,***], Wolfgang Weigand [a,*]

[a] Institute for Inorganic and Analytical Chemistry, Friedrich Schiller Universität Jena, Humboldt Str. 8, 07743, Jena, Germany
[b] Institute of Inorganic Chemistry, Faculty of Chemistry, University of Vienna, Währinger Strasse 42, 1090, Vienna, Austria
[c] Department of Pharmaceutical/Medicinal Chemistry, Institute of Pharmacy, Friedrich Schiller University Jena, Philosophenweg 14, D-07743, Jena, Germany
[d] Research Cluster 'Translational Cancer Therapy Research', University of Vienna, Währinger Strasse 42, 1090, Vienna, Austria

ARTICLE INFO

Keywords:
Pt(IV) prodrugs
NSAIDs
Cyclooxygenase inhibition
Anticancer
Apoptosis

ABSTRACT

In the last decades, inflammation has been recognized as being closely connected to cancer, and joint strategies encompassing chemotherapeutic and anti-inflammatory agents have been extensively studied. In this work, a series of novel cisplatin and oxaliplatin-based Pt(IV) complexes comprising non-steroidal anti-inflammatory drugs (NSAIDs) and their carboxyl ester analogues as axial moieties were synthesized. Several of the cisplatin-based Pt(IV) complexes **22**–**30** showed increased cytotoxicity in the human cancer cell lines CH1/PA-1, SW480 and A549 compared to the Pt(II) drug. For the most potent complex **26,** comprising two aceclofenac (AFC) moieties, the formation of Pt(II)-9-methylguanine (9-MeG) adducts after activation with ascorbic acid (AsA) was proven. Additionally, a significant inhibition of cyclooxygenase (COX) activity and prostaglandin E_2 (PGE_2) production was observed, as well as increased cellular accumulation, depolarization of mitochondrial membranes, and strong proapoptotic potencies in SW480 cells. Overall, these systematic effects shown in vitro confer **26** as a potential anticancer agent combined with anti-inflammatory properties.

1. Introduction

During the last couple of decades, the association between inflammation and oncogenesis has gained enormous attention [1–5]. It has been demonstrated that inflammation predisposes cancer and promotes all stages of tumorigenesis. Cyclooxygenase (COX), a key enzyme in the biosynthesis of prostaglandins derived from arachidonic acid, has crucial functions in promoting inflammation. This enzyme has been identified in three isoforms: COX-1, COX-2, and COX-3, in which COX-3 is characterized as a splice variant of COX-1 at least in dogs. Both COX-1 and COX-2 initialize the catalysis of arachidonic acid to prostaglandins. COX-1 is constitutively expressed in almost all tissues and is responsible for regulation of the basal levels of prostaglandins in normal physiological processes. By contrast, inducible COX-2 is found in inflammatory and tumorigenic tissue, meanwhile, overexpression of prostaglandin E_2 (PGE_2) preferentially mediated by COX-2 is observed [6–10]. In recent studies, it has been shown that PGE_2 plays an important role in cancer development, invasion, metastasis, and drug resistance [6,8–10]. Hence, therapeutic approaches using anticancer agents coupled with anti-inflammatory or COX-inhibiting (especially COX-2) potential have attracted high interest [7,11,12]. Widely used NSAIDs inhibit COX activity, thereby preventing the formation of prostaglandins and their inflammatory effects. At present, several NSAIDs, including aspirin, ibuprofen or celecoxib are under (pre)clinical investigation as single agents or in combination with chemotherapeutic drugs for their cancer prevention and antineoplastic potential [13–15].

Pt(IV) prodrugs with d^6 low-spin octahedral geometry have the potential of overcoming the side effects and drug resistance development

☆ Dedicated to Professor Robert A. Weinberg.

* Corresponding author.
** Corresponding author.
*** Corresponding author. Institute of Inorganic Chemistry, Faculty of Chemistry, University of Vienna, Währinger Strasse 42, 1090, Vienna, Austria.
E-mail addresses: oliver.werz@uni-jena.de (O. Werz), bernhard.keppler@univie.ac.at (B.K. Keppler), wolfgang.weigand@uni-jena.de (W. Weigand).

https://doi.org/10.1016/j.ejmech.2023.115515
Received 23 March 2023; Received in revised form 21 May 2023; Accepted 23 May 2023
Available online 26 May 2023

to the FDA-approved Pt(II) anticancer drugs cisplatin, carboplatin and oxaliplatin [16–20]. In addition, the linked axial ligand(s), which can also possess specific therapeutic properties, can be released as a consequence of intracellular reduction of Pt(IV) prodrugs, making the actual therapeutically active Pt(II) species and its biologically active ligand(s) the perfect combination for a multi-action therapy [17,20–22]. Based on the joint strategy of anticancer and anti-inflammatory potential, a series of multi-specific Pt(IV) complexes with NSAIDs as axial ligands have been designed. For example, naproxen, indomethacin, ibuprofen, flurbiprofen, etc. have been already attached to Pt(IV) complexes, thereby revealing increased anticancer activity [23–30].

Acetylsalicylic acid, also known by its trade name aspirin, has been used as axial ligand for Pt(IV) complexes, which exhibited advantages by significantly enhancing anticancer properties, overcoming drug resistance, and reducing side effects related to ototoxicity [31–33]. However, salicylic acid (SA), an active metabolite of aspirin, has not been used as axial moiety for Pt(IV) prodrugs [34]. Found mainly in willow bark and in a variety of fruits and vegetables, SA was used, historically, as treatment for pain and fever reduction due to its potency to decrease prostaglandin formation by inhibiting COX activity. Hence, SA as well as two salicylate derivatives (salsalate (SSA) and diflunisal (DFS)) were proposed to be attached to the axial positions of Pt(IV) complexes (see Fig. 1). Also, diclofenac (DCF) is a potent anti-inflammatory drug that inhibits COX. In addition to the COX-inhibition-related antiproliferative effects on tumor cells, recent research showed that DCF can alter mitochondrial activities and induce downstream apoptosis-associated events [35–39]. Thus, we designed NSAIDs-linked Pt(IV) complexes comprising DCF, SA, SSA and DFS as axial ligands. Besides, carboxymethyl ester analogues (ASA, ASSA and ADFS) of those NSAIDs were also prepared and used as axial moieties. Aceclofenac (ACF), a carboxymethyl ester of DCF, is known as a potent NSAID and possesses better efficiency and gastrointestinal safety than DCF [40,41]. From the structural perspective, ACF can be taken as a linked conjugate of glycolic acid (GA) and DCF, whereas to suppress prostaglandin formation, ACF is selectively inhibiting COX-2 and DCF inhibits COX-1 and COX-2 with relatively low potency [40,41]. In view of synthesis strategy, ligands with a terminal carboxylic acid group can be directly attached to Pt(IV) precursors, which can be achieved by linking the free ligands in the presence of coupling agents to Pt(IV), or by reaction with activated forms of the ligands, including *N*-hydroxysuccinimide (NHS) esters, anhydrides or acyl chlorides. For ligands without a carboxylic acid group, a linker or spacer unit such as succinic acid, *N*,*N*′-disuccinimidyl carbonate (DSC) or glycolic acid (GA) was attached, followed by tethering them to the axial position of Pt(IV) precursors. The approach of linking a spacer to the onsite carboxylic acid group to form a second carboxylic acid group is a blind spot and has not been reported so far. After submission of this manuscript, Aldrich-wright and co-workers reported three mono-substituted Pt(IV) complexes bearing one acemetacin as an axial ligand. Like ACF, acemetacin is also a commercially available NSAID and can be considered as a conjugate of indometacin with GA [42]. Based on those strategies, twelve Pt(IV) complexes (**22**–**31** and **33**) were synthesized and thoroughly characterized using spectroscopic techniques. The antiproliferative effects on a panel of three different cancer cell lines (CH1/PA-1, SW480 and A549) and COX inhibition in A549 cells were studied. For the most potent complexes **24** and **26,** a series of additional biological investigations was conducted to elucidate the underlying mechanisms of action.

2. Results and discussion

2.1. Synthesis and characterization

The syntheses of carboxymethyl ester analogues **9**–**11** and Pt(IV) compounds **22**–**34** are summarized in Scheme 1. The structures of these Pt(IV) complexes were characterized by NMR spectroscopy (^{1}H, ^{13}C, ^{19}F and ^{195}Pt), mass spectrometry and elemental analysis (see experimental section). Briefly, the Pt(IV) precursors oxoplatin and dihydroxido oxaliplatin were obtained through oxidation with hydrogen peroxide (w/w, 30%) of cisplatin and oxaliplatin. NSAIDs (**1**–**4**) were activated with NHS resulting in esters (**12**–**15**), followed by the reaction with oxoplatin and dihydroxido oxaliplatin in order to gain the mono-substituted complexes **22**–**25** and **31**, respectively. Mixing complexes **22** and **31** with acetic anhydride generated complexes **30** and **32**, respectively. The attempt to synthesize di-substituted Pt(IV) complexes with two DCF moieties was not successful, as a lactam (diclofenac amide) featuring a steady five-membered ring was always formed when using general synthetic routes to prepare DCF anhydride or acyl chloride (simply using higher equivalents of DCF-NHS did not work; see below). In order to generate the bis-DCF Pt(IV) complexes, 6-aminohexanoic acid containing a terminal amino group was selected as a linker, which is similar to previous studies [43,44]. First, boc-protected Pt(IV) complex **33** was obtained by a reaction between dihydroxido oxaliplatin(IV) and **21**, which was then deprotected to form **34** through the conjugation between the released terminal amine group and **12**. However, in the case of oxoplatin, this synthetic approach did not work. Alternatively, when processing of ACF (**8**), which contains an extended carboxylic acid group by conjugation with glycolic acid, the formation of mentioned above lactam can be avoided. During the synthetic process, the di-substituted Pt(IV) complex **26** was surprisingly obtained by a reaction between the NHS-activated ACF (**16**) and oxoplatin. Then, the same strategy was expanded to compounds **2**–**4,** resulting in the generation of **9**–**11**. Subsequently, after activation with NHS, the yielded compounds **17**–**19** were reacted with oxoplatin to produce the di-substituted Pt(IV) complexes **27**–**29**.

The synthesis of di-substituted Pt(IV) complexs using NHS esters has been rarely reported [45]. Interestingly, we observed a distinctly accelerated reaction rate when using the NHS ester of the linked GA compared to the unmodified NHS-NSAIDs. This difference was proven by monitoring the reaction process with ^{1}H NMR. In Fig. 2, the reaction of oxoplatin with 1.1 eq of ACF-NHS (Fig. 2a) or DCF-NHS (Fig. 2b) in DMSO-d_6 at 50 °C is shown. After 1 h, the reaction solution with ACF-NHS became clear, which suggested that oxoplatin was consumed completely (the signal of the ammine for mono-substituted Pt(IV) species was found at 5.94 ppm). However, the solution with DCF-NHS was still turbid, indicating that the reaction was not finished within 1 h (Fig. 2c). Therefore, one more equivalent of NHS esters was added to the

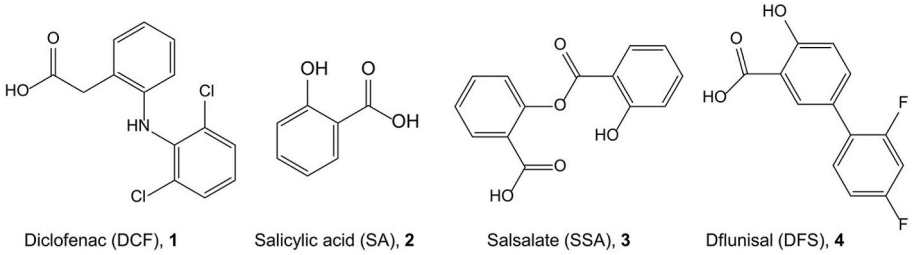

Fig. 1. Non-steroidal anti-inflammatory drugs (NSAIDs) used in this paper.

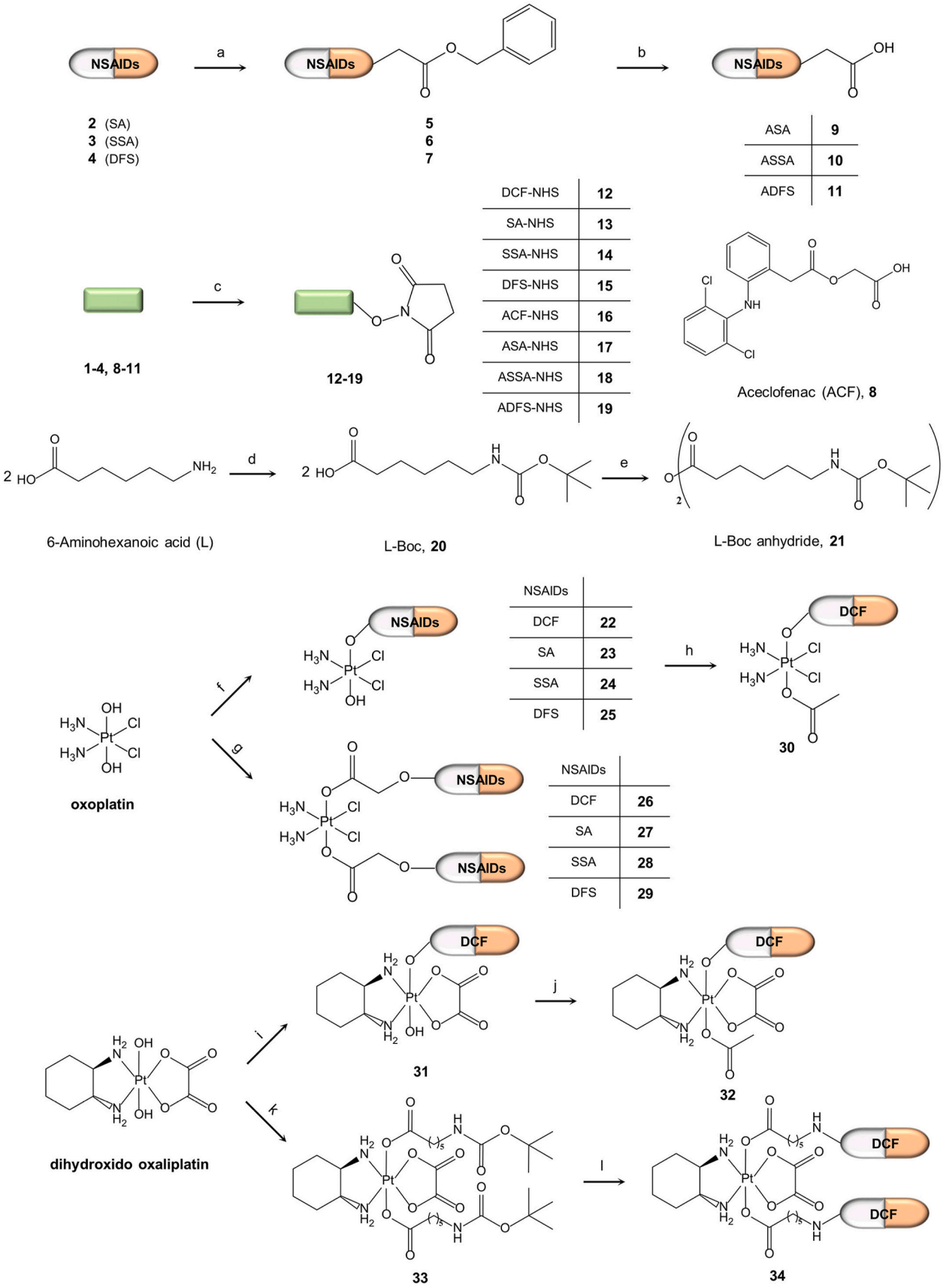

Scheme 1. General overview of synthesis routes. Regents and conditions: (a) benzyl chloroacetate, TEA, acetone, 50 °C, 24 h; (b) H_2, Pd/C (10%), DCM, rt, overnight; (c) NHS, DCC, DCM, overnight; (d) di-*tert*-butyl dicarbonate (Boc anhydride) , TEA, acetone-H_2O, rt, 4 h; (e) DCC, DCM, rt, overnight; (f) NHS esters (**12**–**15**), DMSO, 50 °C, overnight; (g) NHS esters (**16**–**19**), DMSO, 50 °C, 2 d; (h) acetic anhydride, DMF, rt, overnight; (i) DCF-NHS, DMSO, 50 °C, overnight; (j) acetic anhydride, DMF, rt, overnight; (k) L-Boc anhydride **21**, DMF, rt, 4 d; (l) *i*) excess TFA, DCM, rt, 3 h; *ii*) DCF-NHS, TEA, DMF, rt, overnight.

Table 1
Cytotoxicity of **22**–**32** and **34** compared to cisplatin and oxaliplatin in three human cancer cell lines. IC_{50} values are means ± standard deviations from at least three independent experiments (MTT assay, 96 h exposure).

Complex	IC_{50} (μM) ± SD		
	CH1/PA-1	SW480	A549
22	0.0091 ± 0.0020	0.14 ± 0.03	0.35 ± 0.04
23	0.052 ± 0.006	0.16 ± 0.04	2.9 ± 0.7
24	0.073 ± 0.012	0.082 ± 0.024	2.0 ± 0.7
25	0.033 ± 0.006	0.20 ± 0.07	1.1 ± 0.3
26	0.015 ± 0.003	0.070 ± 0.019	0.26 ± 0.06
27	0.032 ± 0.001	0.31 ± 0.06	1.4 ± 0.1
28	0.014 ± 0.002	0.14 ± 0.02	0.48 ± 0.14
29	0.022 ± 0.005	0.15 ± 0.02	0.66 ± 0.08
30	0.011 ± 0.003	0.12 ± 0.03	0.34 ± 0.02
cisPt	0.056 ± 0.002	2.6 ± 0.4	2.7 ± 0.2
31	0.41 ± 0.10	1.3 ± 0.1	4.9 ± 0.7
32	0.12 ± 0.01	0.50 ± 0.19	2.1 ± 0.5
34	0.10 ± 0.02	2.6 ± 1.1	>200
oxaliPt	0.11 ± 0.02	0.35 ± 0.07	1.3 ± 0.2

solution to complete the reaction. As the reaction time increased for the ACF-NHS ester, also the ammine signal for the di-substituted species was detected at 6.52 ppm, concomitant with a decrease of the peak at 5.94 ppm (Fig. 2a). After 45 h and addition of two more equivalents of ACF-NHS the mono-substituted Pt(IV) species at 5.94 ppm eventually disappeared (Fig. 2a). In contrast to ACF-NHS, when using DCF-NHS only small amounts of di-substituted species could be observed even after longer reaction times and excess ester (Fig. 2b). Therefore, the linkage of GA accelerated the formation of mono-substituted Pt(IV) complex and furthermore also allowed for the preparation of di-substituted species using NHS esters.

2.2. Cytotoxicity

Cytotoxicity of Pt(IV) complexes **22**–**32** and **34** was determined in CH1/PA-1 (ovarian teratocarcinoma), SW480 (colon carcinoma), and A549 (non-small-cell lung carcinoma) cell lines by the metabolic MTT assay. The IC_{50} values (= concentrations of substance which result in a number of viable cells equal to 50% of untreated controls) are reported in Table 1 and concentration-effect curves are shown in Figs. S1–S3. To exclude artifacts resulting from possible direct interactions between the compounds and mitochondrial metabolism, four of the more potent compounds were spot-checked in a single neutral red assay experiment in CH1/PA-1 cells, with results deviating negligibly from MTT-based results (data not shown).

Especially in the broadly chemosensitive CH1/PA-1 cells, cisplatin-based complexes **22**–**30** possessed the strongest potency. They showed lower IC_{50} values than cisplatin, except for complexes **23** and **24** in A549 and CH1/PA-1 cells, respectively. Among the homologous mono-substituted complexes **22**–**25**, the DCF-bearing complex **22** was the most potent in two of the three cell lines. Otherwise, there is no universally valid rank order of cytotoxicity with respect to the variable axial ligand. ACF (the carboxymethyl ester derivative of DFC) yielded the most cytotoxic complex **26** (in two of three cell lines) among the di-substituted homologues **26**–**29**, whereas the carboxymethyl ester of SA yielded the least cytotoxic (**27**), being roughly 2–5 times less potent than **26**. Notably, the most effective complex **26** in SW480 and A549 cells showed 37-fold and 10-fold higher cytotoxicity than cisplatin. Replacing the hydroxido ligand of **22** with an acetato ligand (complex **30**) had virtually no consequences for cytotoxicity.

Oxaliplatin-based complexes **31**, **32** and **34** had comparable or higher IC_{50} values than those of oxaliplatin in the three cell lines, with an axial acetato ligand (complex **32**) being slightly but consistently advantageous over a hydroxido ligand (complex **31**) in this case. Furthermore, **31** and **32** are overall by roughly one order of magnitude less potent than their cisplatin-based analogues **22** and **30**, respectively. Surprisingly though, complex **34** bearing two linker-coupled DCF moieties turned out to be completely inactive in A549 cells, while retaining activity in the other two cell lines.

2.3. Inhibition of PGE_2 formation in A549 cells

Due to up-regulated COX-2 expression in cancer cells, an increased level of PGE_2 is frequently detected in the tumor environment.

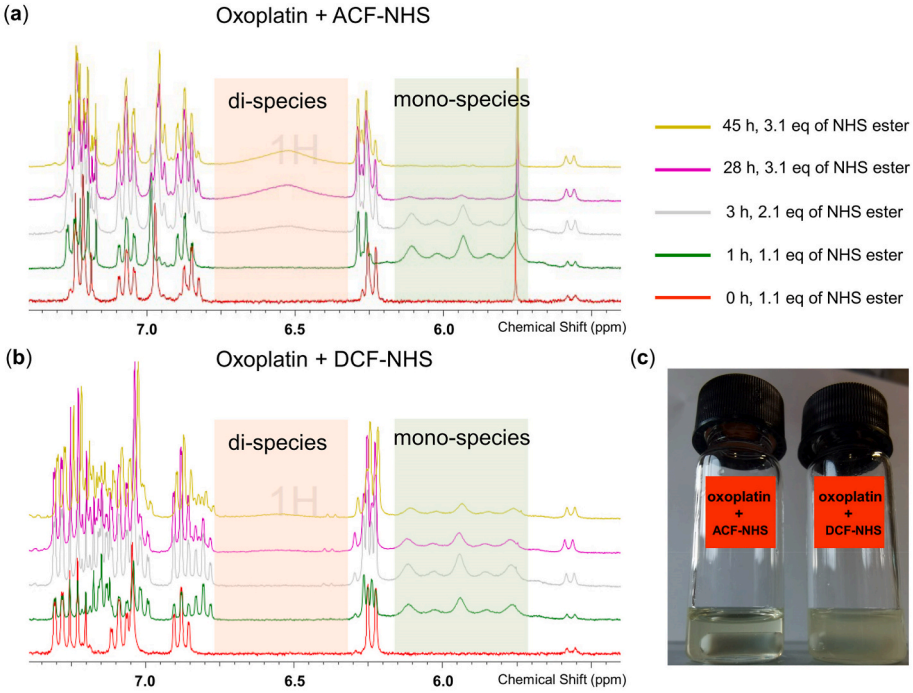

Fig. 2. Selected area of time-dependent ^{1}H NMR spectra of reaction process of (a) oxoplatin with ACF-NHS; (b) oxoplatin with DCF-NHS; (c) the picture of reaction solutions with two NHS esters (1.1 eq) after 1 h.

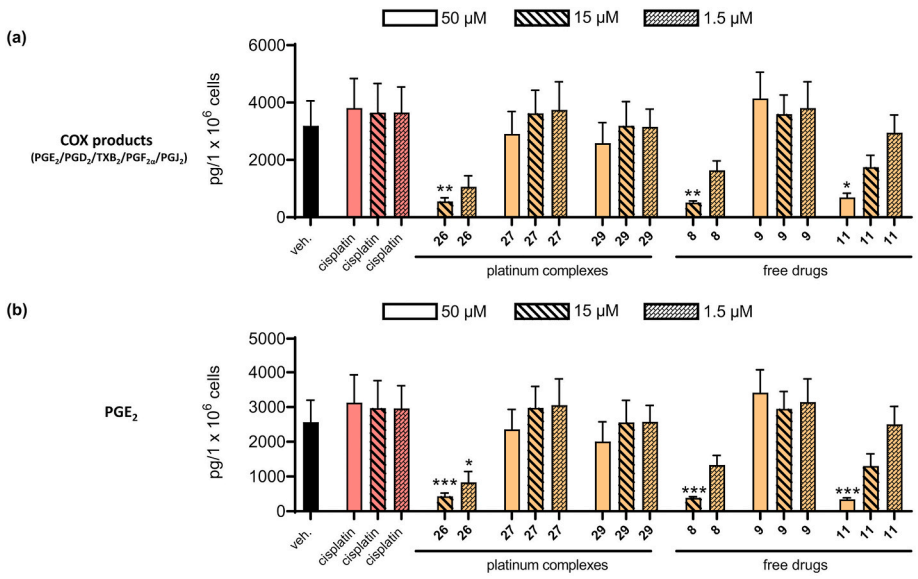

Fig. 3. Inhibition of COX product formation by compounds **8**, **9**, **11**, **26**, **27** and **29** in A549 cells. A549 cells were preincubated with 2 ng/mL IL-1β for 24 h and then treated with either vehicle (veh., containing 0.1% DMSO), cisplatin, Pt(IV) complexes (**26**, **27** and **29**) or the free drugs (**8**, **9**, **11**) for 15 min and then stimulated with 2.5 μM Ca^{2+}-ionophore A23187 to induce COX product formation for 10 min at 37 °C. COX products were then purified by solid-phase extraction and analyzed by UPLC-MS/MS. Values are given as COX products (PGE_2, PGD_2, TXB_2, $PGF_{2\alpha}$ and PGJ_2) in pg/10^6 A549 cells in (a) for COX product levels (the sum of PGE_2, PGD_2, TXB_2, $PGF_{2\alpha}$ and PGJ_2) or (b) for PGE_2 levels alone, after exposure to compounds **8**, **9**, **11**, **26**, **27** and **29**. Data are means ± SEM, n = 3; Data were log-transformed for statistical analysis; $^*p < 0.05$, $^{**}p < 0.01$, $^{***}p < 0.001$, one-way ANOVA with Dunnett's multiple comparisons test against DMSO control.

Additionally, many studies suggest that COX-2-derived PGE_2 is capable of increasing tumor proliferation and invasion, promoting metastasis and angiogenesis, as well as suppressing antitumor immunity [9,10]. The aim of this work is to combine anticancer and anti-inflammatory properties; hence, we studied the effect of di-substituted Pt(IV) complexes (**26**, **27** and **29**) and their corresponding free drugs (**8**, **9** and **11**) on the levels of COX-mediated products including PGE_2, PGD_2, PGJ_2, $PGF_{2\alpha}$, and thromboxane B_2 (TXB_2) (Fig. 3a) as well as PGE_2 levels alone (Fig. 3b) in A549 cells at concentrations of 1.5, 15 and 50 μM. To induce COX-2 expression, A549 cells were first treated with 2 ng/mL IL-1β for 24 h, test compounds were added, and cells were then stimulated with 2.5 μM Ca^{2+}-ionophore A23187 for 10 min to induce COX product formation. Compared to the vehicle control and cisplatin groups, the most cytotoxic complex **26** as well as its free ligand **8** (= ACF), showed significant inhibition of COX activity, as the levels of COX products were remarkably decreased in a concentration-dependent manner (Fig. 3a). Even at the lowest tested concentration of 1.5 μM, the inhibition by **26** and **8** achieved up to 70%. Moreover, compound **11** exhibited a similar concentration-dependent inhibition; however, the inhibition by its corresponding Pt(IV) species **29** did not parallel the inhibitory efficiency of **11** with increasing concentrations. The least cytotoxic di-substituted complex **27** and its ligand **9** did not show noteworthy COX inhibition, except that **27** was slightly (though not significantly) inhibitory at the highest tested concentration. In general, the potency of COX inhibition seems to correlate with the cytotoxicity profiles in A549 cells in the following order: **26** > **29** > **27**. As depicted in Fig. 3b, compounds **8** and **26** remarkably reduced PGE_2 production. PGE_2 plays a pivotal role in the migration of cancer cells, and high expression of COX-2 in tumor tissue can lead to dysfunction of the antitumor immune response through PGE_2. The inhibition of COX-2 and secretion of PGE_2 suggest that complex **26** potentially can hamper tumor progression and alter the immune microenvironment of cancer cells. However, it should be mentioned that the inhibition of PGE_2 formation in A549 cells was measured within 1 h, whereas cytotoxicity was determined after 96 h, suggesting that COX inhibition and cytotoxicity may act independently.

2.4. Stability

The stability of complex **26** in DMF(d_7)-PBS (phosphate-buffered saline, in D_2O, pH = 7.4) (v/v; 4/1) at 37 °C was examined using ^1H NMR spectroscopy. As displayed in Fig. S4, the ^1H NMR spectra were checked at different incubation times. After 48 h, no new peaks or species were observed. As a reference, compound **8** was checked under the same conditions, and hydrolysis of the linked GA was not observed. In general, compounds **8** and **26** are stable under the tested conditions.

2.5. Reduction with ascorbic acid

Pt(IV) complexes working as prodrugs are proposed to release active Pt(II) species under intracellular reduction. Thus, the reduction of complex **26** was studied using ascorbic acid (AsA) as a reducing agent. The ^{195}Pt NMR spectra were evaluated after incubation of complex **26** in the presence of AsA (10 eq) in DMF-PBS (v/v; 4/1) at 37 °C for 18 h. The signal of Pt(IV) disappeared during incubation. At the same time, the peak for Pt(II) was observed at −2097 ppm, which was in agreement with that of cisplatin (Fig. 4) [46].

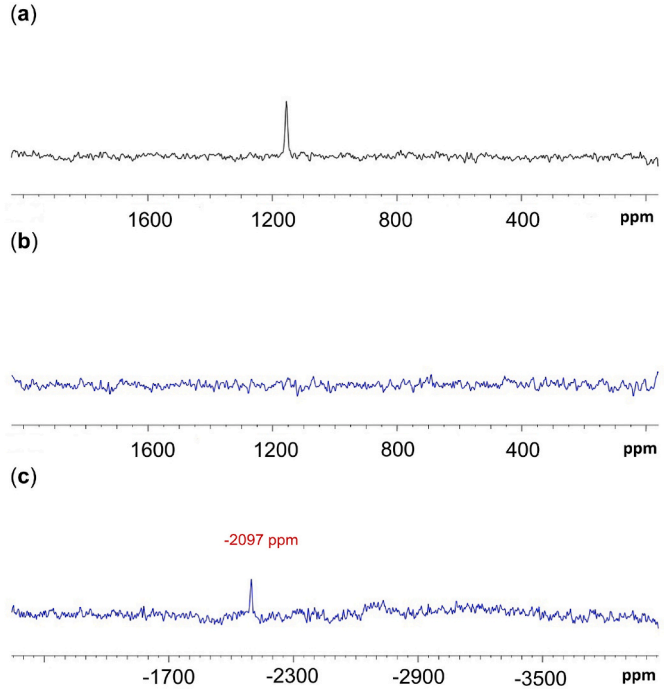

Fig. 4. ^{195}Pt NMR spectra of complex **26** in DMF-PBS (v/v; 4/1) (a) before adding AsA; (b and c) after adding AsA (10 eq), the solution was incubated at 37 °C for 18 h.

2.6. 9-Methylguanine binding experiment

It is well-known that the mechanism of action of cisplatin involves the crosslinking of DNAbases by formation of DNA-Pt adducts, preventing repair of the DNA, finally leading to DNA damage and subsequently inducing apoptosis in cancer cells. The crosslinks normally occur on the N_7 position of guanine [22]. Thus, we investigated DNA binding using 9-methylguanine (9-MeG) as a simple model. Complex **26** was incubated with 9-MeG (3 eq) in the presence of AsA (10 eq) at 37 °C for 24 h. Two peaks with *m/z* 430.02 (t_R = 1.07 min) and *m/z* 577.97 (t_R = 1.65 min), which can be assigned to the adducts $[(Pt(NH_3)_2(9\text{-MeG})Cl)]^+$ and $[(Pt(NH_3)(9\text{-MeG})_2Cl)]^+$, respectively, were found in the LC-ESI(+)-MS spectrum (Fig. S5). Comparable adducts were also found when incubating cisplatin with 9-MeG under the same conditions [46].

2.7. Cellular accumulation

It has been demonstrated that increased lipophilicity within homologous series of Pt(IV) complexes may lead to enhanced cellular accumulation via passive diffusion [47]. Generally, conjugation with hydrophobic ligands leads to enhanced lipophilicity. Thus, the most potent cytotoxic complexes, in respect to the lowest IC_{50} values in the colon carcinoma cell line SW480, were chosen for evaluation of cellular accumulation, depolarization of the mitochondrial membranes as well as for induction of apoptosis: **24**, as a mono-substituted salicylate complex, and **26**, as a di-substituted diclofenac complex. As shown in Fig. S6, the cellular accumulation of complex **26** (448 fg platinum/cell), being the more lipophilic complex, is approximately 2.3-fold higher compared to the mono-substituted complex **24** (191 fg platinum/cell). Cisplatin, as the reference compound, with a cellular accumulation of 12 fg platinum/cell, demonstrated a significant lower uptake under essentially similar experimental conditions [48].

2.8. Depolarization of mitochondrial membranes and induction of apoptosis

NSAIDs have been reported to induce mitochondrial dysfunction, especially changes that affect the mitochondrial membrane potential (ΔΨm). The collapse of the ΔΨm may lead to the opening of the mitochondrial permeability transition pores and subsequent release of cytochrome *c*, which in turn triggers downstream events such as apoptosis. To assess the condition of mitochondrial membrane potentials in a cell population, SW480 cells were treated with complexes **24** and **26** and stained with JC-1, which is a membrane-permeable lipophilic cationic fluorochrome showing potential-dependent accumulation in mitochondria. As illustrated by Fig. 5a, concentration-dependent mitochondrial damage upon incubation with **26** for 24 h was observed. At a concentration of 5 μM, 35% of cells with depolarized mitochondria were observed; by increasing the concentration to 25 μM, the value went up to 89%. In the case of complex **24** at the same concentrations, the values were only 1% and 17%, respectively, implying that **26** is much more potent than **24** (Fig. S7).

The induction of cell death by complexes **24** and **26** was investigated using a flow-cytometric annexin V-FITC/propidium iodide (PI) double staining assay in the colon cancer line SW480 with concentrations of 0.2, 1.0, 5.0 and 25 μM (Fig. 5b, c and Fig. S8). Complexes **24** and **26** induced concentration-dependent increases in necrosis, as well as in early and late apoptosis. After exposure for 24 h at a concentration of 25 μM, 13.2% and 51.8% of cells were induced to enter late apoptosis, respectively. This is

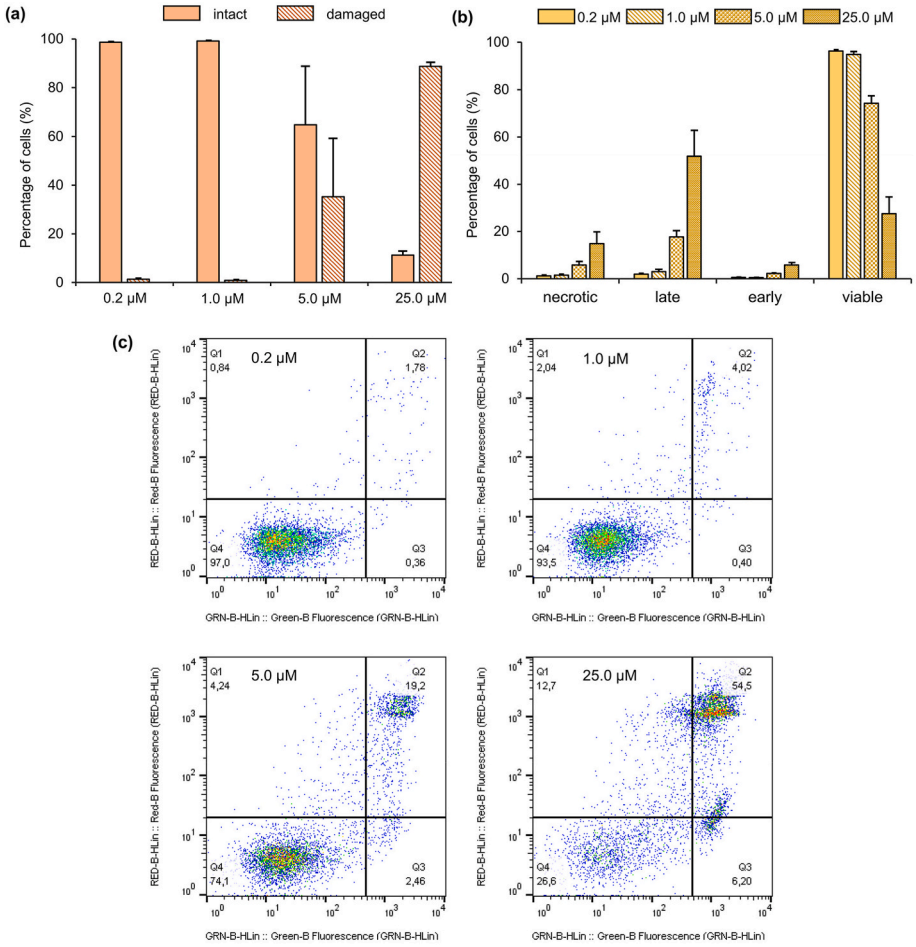

Fig. 5. Flow cytometry analysis of SW480 cells upon treatment with complex **26** for 24 h. (a) Percentage of cells with depolarized mitochondria according to the JC-1 assay after treatment with 0.2, 1.0, 5.0 or 25 μM of **26**. Values are means ± SDs of triplicate experiments. (b) Percentage of necrotic, late apoptotic, early apoptotic, and viable cells according to the annexin V-FITC/PI assay upon treatment at different substance concentrations. (c) Exemplary dot plot analysis from the latter assay (one out of three independent experiments for each of the four concentrations). Dots represent necrotic (Q1, upper left quadrant), late apoptotic (Q2, upper right), early apoptotic (Q3, lower right) and viable cells (Q4, lower left).

particularly remarkable as we have previously found that treatment with 100 μM of cisplatin causes only less than 3% of SW480 cells to enter late apoptosis after 24 h [49], which suggests that complexes 24 and 26 have manifold higher pro-apoptotic effects than cisplatin.

3. Conclusion

In summary, a series of Pt(IV) complexes comprising NSAIDs or their carboxymethyl ester analogues as axial ligands are described with regard to their synthesis and structural characterization. Di-substituted Pt (IV) complexes were synthesized through NHS esters linked via glycolic acid, providing an alternative synthesis route for Pt(IV) complexes. Overall, cisplatin-based Pt(IV) complexes showed increased cytotoxicity in three human cancer cell lines. Among them, complex **26** (containing two axial aceclofenac ligands) was most potent in SW480 and A549 cells and was up to 37-fold and 10-fold more cytotoxic than cisplatin. A reduction study of **26** in the presence of ascorbic acid proved that it can be used as a prodrug that becomes activated upon reduction by biologically relevant reductants. Furthermore, two Pt(II)-9-MeG adducts were found when the complex was exposed to 9-MeG in the presence of ascorbic acid, suggesting the possibility of Pt(II)-DNA cross-link formation, analogous to the mode of action of cisplatin. Compared to the parent drug cisplatin, enhanced cellular accumulation and a manifold increased apoptosis-inducing potency of **26** in SW480 cells were observed. To investigate the combined anticancer and anti-inflammatory strategy, the ability of COX inhibition was explored by assessment of prostaglandin formation in A549 cells. The levels of COX-derived prostanoids were remarkably reduced by the treatment with complex **26** or its axial ligand ACF (compound **8**); moreover, the suppression of PGE_2 alone occurred essentially to the same extent. Altogether, Pt(IV) prodrug **26** with two aceclofenac moieties as axial ligands possesses potential as a promising antitumor agent with enhanced cellular accumulation, high apoptosis-inducing potency and outstanding COX-inhibiting properties.

4. Experimental section

4.1. Materials and methods

4.1.1. Chemical agents

All the reagents and solvents were of analytical grade and were used without further purification. Potassium tetrachloroplatinate(II) was donated from Umicore Hanau. *N,N′*-Dicyclohexylcarbodiimide (DCC) was purchased from Carl Roth GmbH. Benzyl chloroacetate, 2-(2,6-dichloroanilino)phenylacetic acid, 2-carboxyphenyl salicylates, *N*-hydroxysuccinimide (NHS) and di-*tert*-butyl dicarbonate were purchased from TCI Deutschland GmbH. Anhydrous DMSO and anhydrous DMF were obtained from Sigma-Aldrich and Alfa Aesar Thermo Fisher Scientific, respectively. 6-Aminocaproic acid was obtained from Fluka Chemie GmbH. All solvents were dried and distilled prior to use according to standard methods.

4.1.2. Instruments

The ^{1}H,$^{13}C\{^{1}H\}$, $^{19}F\{^{1}H\}$ and ^{195}Pt NMR spectra were recorded with Bruker Avance 300 MHz, 400 MHz and 600 MHz spectrometers at 297 K. Chemical shifts are given in parts per million with references to internal $SiMe_4$ (^{1}H, ^{13}C), to external K_2PtCl_4 (^{195}Pt), and to external trifluorotoluene (^{19}F). The mass spectrum was recorded with Bruker (Bremen, Germany) MAXIS mass spectrometer. Elemental analysis was performed with a Leco CHNS-932 apparatus. TLC was performed by using Merck TLC aluminium sheets (silica gel 60 F254). Geduran Si 60 (0.063–0.200 mm) was used as the stationary phase for column chromatography.

4.1.3. Single-crystal X-ray structural analyses

The single-crystal X-ray intensity data for compounds **5** and **15** were collected on a Bruker-Nonius Kappa-CCD diffractometer equipped with a Mo-Kα IμS microfocus source and an Apex2 CCD detector, at $T = 120$ (2) K. The crystal structures were solved with SHELXT-2018/3 [50] and refined by full matrix least-squares methods on F^2 with SHELXL-2018/3 [51], using the Olex 1.2 environment [52]. Multi-scan absorption correction was applied to the intensity data [53]. CCDC 2241070 (for compound **5**) and 2219838 (for compound **15**) contain the supplementary crystallographic data for this paper. These data can be obtained free of charge from The Cambridge Crystallographic Data Centre (CCDC; http://www.ccdc.cam.ac.uk).

4.1.4. Cell lines and media

CH1/PA-1 cells (identified via STR profiling as PA-1 ovarian teratocarcinoma cells by Multiplexion, Heidelberg, Germany) were a gift from Lloyd R. Kelland, CRC Center for Cancer Therapeutics, Institute of Cancer Research, Sutton, UK. SW480 (human adenocarcinoma of the colon) and A549 (human non-small cell lung cancer) cells were provided by the Institute of Cancer Research, Department of Medicine I, Medical University of Vienna, Austria. All cell culture media, supplements and assay reagents were purchased from Sigma-Aldrich, and plasticware from Starlab unless noted otherwise. Cells were grown in 75 cm^2 culture flasks as adherent cultures in minimum essential medium (MEM) supplemented with 10% heat-inactivated fetal bovine serum (FBS; BioWest), 1 mM sodium pyruvate, 4 mM L-glutamine, and 1% non-essential amino acids (from 100 × ready-to-use stock). Cultures were maintained at 37 °C in a humidified atmosphere containing 5% CO_2.

4.2. Synthesis of compounds

4.2.1. General procedure a for the preparation of benzyloxy carbonyl methyl esters 5–7

Benzyl chloroacetate (1 mmol) was added dropwise to a solution of corresponding acids **2**–**4** (1.1 mmol) and triethylamine (1.5 mmol) in 10 ml of acetone. The solution was heated to 50 °C for 24 h. Then, the mixture solution was filtered and dried using a rotary evaporator.

4.2.1.1. 2-Oxo-2-(phenylmethoxy)ethyl 2-hydroxybenzoate (5) SA-GA-Bn. Purification via column chromatography (SiO_2, DCM) to give **5** as a white solid (yield, 66%). $R_f = 0.71$ (DCM). The single crystal of compound **5** was obtained by slow evaporation of solution in DCM at room temperature. The molecular structure was determined by using X-ray crystallography (see Table S1 and Fig. S. 75).

^{1}H NMR (400 MHz, $CDCl_3$): δ 10.39 (s, 1H), 7.93 (dd, $J = 8.0$, 1.6 Hz, 1H), 7.49 (t, $J = 7.4$ Hz, 1H), 7.38–7.34 (m, 5H), 6.99 (d, $J = 8.0$ Hz, 1H), 6.91 (t, $J = 7.6$ Hz, 1H), 5.25 (s, 2H), 4.91 (s, 2H) ppm.

$^{13}C\{^{1}H\}$ NMR (101 MHz, $CDCl_3$, 297 K): δ 169.3, 167.2, 161.8, 136.3, 135.0, 130.2, 128.7128.6, 128.4, 119.4, 117.7, 111.6, 67.3, 61.2 ppm.

Anal Calc. for $C_{16}H_{14}O_5$: C, 67.13; H, 4.93%. Found: C, 67.06; H, 4.95%.

4.2.1.2. 2-Oxo-2-(phenylmethoxy)ethyl (2-((2-hydroxybenzoyl)oxy)benzoate) (6) SSA-GA-Bn. Purification via column chromatography (SiO_2, EtOAc/cyclohexane = 1/5) to give **6** as a white solid (yield, 58%). $R_f = 0.27$ (EtOAc/cyclohexane = 1/5).

^{1}H NMR (400 MHz, CD_2Cl_2): δ 10.27 (s, 1H), 8.17 (dd, $J = 7.9$, 1.6 Hz, 1H), 8.11 (dd, $J = 8.0$, 1.6 Hz), 7.71 (td, $J = 7.8$, 1.6 Hz, 1H), 7.57 (t, $J = 7.8$ Hz, 1H), 7.46 (t, $J = 7.6$ Hz, 1H), 7.36–7.31 (m, 5H), 7.05 (d, $J = 8.4$ Hz, 1H), 6.99 (t, $J = 7.6$ Hz, 1H), 5.16 (s, 2H), 4.76 (s, 2H) ppm.

$^{13}C\{^{1}H\}$ NMR (101 MHz, CD_2Cl_2): δ 169.2, 167.6, 163.9, 162.4, 150.6, 136.9, 135.7, 134.9, 132.5, 131.1, 128.9, 128.8, 128.6, 127.1, 124.4, 123.0, 119.9, 118.0, 112.4, 67.4, 61.7 ppm.

Anal Calc. for $C_{23}H_{18}O_7$: C, 67.98, H, 4.46%. Found: C, 68.03; H, 4.41%.

4.2.1.3. 2-Oxo-2-(phenylmethoxy)ethyl 2′,4′-difluoro-3-hydroxy[1,1′-biphenyl]-4-carboxylate (7) DFS-GA-Bn. Purification via column chromatography (SiO_2, EtOAc/cyclohexane = 1/5) to give **7** as a white solid (yield, 58%). R_f = 0.43 (EtOAc/cyclohexane = 1/5).

^{1}H NMR (400 MHz, $CDCl_3$): δ 10.46 (s, 1H), 8.06 (s, 1H), 7.69–7.60 (m, 1H), 7.44–7.30 (m, 6H), 7.08 (d, J = 8.7 Hz, 1H), 7.00–6.85 (m, 2H), 5.25 (s, 2H), 4.93 (s, 2H).

^{13}C{^{1}H} NMR (101 MHz, $CDCl_3$): δ 169.2 (s), 167.1 (s), 163.5 (d, J = 11.8 Hz), 161.4 (s), 160.9 (dd, J = 11.8, 5.5 Hz), 158.4 (d, J = 11.9 Hz), 136.8 (d, J = 3.1 Hz), 134.9 (s), 131.1 (dd, J = 9.5, 4.8 Hz), 130.4 (d, J = 2.6 Hz), 128.7 (d, J = 3.3 Hz), 128.4 (s), 126.4 (s), 124.0 (dd, J = 13.6, 3.9 Hz), 118.0 (m), 111.5 (d, J = 3.8 Hz), 104 (t, J = 26.0 Hz), 67.4 (s), 61.3 (s) ppm.

^{19}F{^{1}H} NMR (376 MHz, $CDCl_3$): δ −111, −114 ppm.

Anal Calc. for $C_{22}H_{16}O_5F_2$: C, 66.33; H, 4.05%. Found: C, 66.13; H, 4.08%.

*4.2.2. General procedure B for the preparation of carboxymethyl esters **9**–**11***

Corresponding benzyloxy carbonyl methyl esters **5**–**7** (1 mmol), Pd/C (10 wt% loading, 7.3% mol) and dichloromethane (10 ml) were mixed in the flask. Remove O_2 in the solvent and air inside the flask by hydrogen (H_2) bubbling using a H_2-filled double-layered rubber balloon. Then the mixture solution was stirred overnight under hydrogen atmosphere at room temperature. After filtration through Celite, the filtrate was dried by a rotary evaporator and the appropriate product was obtained as a solid.

4.2.2.1. 2-(2-Hydroxybenzoyl)oxyacetic acid (9) SA-GA. Compound **9** was obtained as a reddish solid (yield, 88%).

^{1}H NMR (400 MHz, $CDCl_3$): δ 10.35 (br s, 1H), 7.92 (dd, J = 8.0, 1.3 Hz, 1H), 7.50 (t, J = 7.8 Hz, 1H), 7.00 (d, J = 8.5 Hz, 1H), 6.92 (t, J = 7.6 Hz, 1H), 4.93 (s, 2H) ppm.

^{13}C{^{1}H} NMR (101 MHz, $CDCl_3$): δ 172.7, 169.2, 161.8, 136.5, 130.2, 119.5, 117.7, 111.4, 60.5 ppm.

Anal Calc. for $C_9H_8O_5$: C, 55.11; H, 4.11%. Found: C, 55.00; H, 4.13%.

4.2.2.2. 2-(2-((2-Hydroxybenzoyl)oxy)benzoate)oxyacetic acid (10) SSA-GA. Compound **10** was obtained as a white solid (yield, 88%).

^{1}H NMR (400 MHz, CD_2Cl_2): δ 8.15 (d, J = 7.7 Hz, 1H), 8.10 (d, J = 7.9 Hz, 1H), 7.70 (t, J = 7.7 Hz, 1H), 7.54 (t, J = 7.8 Hz, 1H), 7.45 (t, J = 7.6 Hz, 1H), 7.30 (d, J = 8.1 Hz, 1H), 7.03–6.97 (m, 2H), 4.75 (s, 1H) ppm.

^{13}C{^{1}H} NMR (101 MHz, CD_2Cl_2): δ 172.3, 168.7, 163.5, 161.9, 150.1, 136.5, 134.6, 132.1, 130.6, 126.7, 124.0, 122.4, 119.6, 117.6, 111.9, 60.7 ppm.

Anal Calc. for $C_{16}H_{12}O_7$: C, 60.76; H, 3.82%. Found: C, 60.43; H, 3.84%.

4.2.2.3. 2-(2′,4′-difluoro-3-hydroxy[1,1′-biphenyl]-4-carboxylate)oxyacetic acid (11) DFS-GA. Compound **11** was obtained as a light grey solid (yield, 94%).

^{1}H NMR (400 MHz, $CDCl_3$): δ 10.42 (br s, 1H), 8.05 (s, 1H), 7.64 (dd, J = 8.7, 1.7 Hz, 1H), 7.37 (td, J = 8.7, 6.5 Hz, 1H), 7.08 (d, J = 8.7 Hz, 1H), 7.01–6.85 (m, 2H), 4.94 (s, 2H) ppm.

^{13}C{^{1}H} NMR (101 MHz, $CDCl_3$): δ 172.0 (s), 169.1 (s), 163.5 (d, J = 11.9 Hz), 161.4 (s), 161.0 (dd, J = 11.8, 8.5 Hz), 158.5 (d, J = 11.9 Hz), 137.0 (d, J = 3.0 Hz), 131.1 (dd, J = 9.5, 4.8 Hz), 130.3 (d, J = 2.6 Hz), 126.4 (s), 123.9 (d, J = 13.7 Hz), 118.1 (s), 111.7 (dd, J = 21.1, 3.7 Hz), 104.4 (t, J = 26.0 Hz), 60.6 (s) ppm.

^{19}F{^{1}H} NMR (376 MHz, $CDCl_3$): δ −111, −114 ppm.

Anal Calc. for $C_{15}H_{10}O_5F_2$: C, 58.45; H, 3.27%. Found: C, 58.16; H, 3.28%.

*4.2.3. General procedure C for the preparation of NHS esters **12**–**19***

Dicyclohexylcarbodiimide (DCC, 1.5 mmol) was added to a solution of corresponding acids **1**–**4** and **8**–**11** (1.0 mmol) and NHS (1.3 mmol) in 6 ml of dichloromethane. The solution was kept stirring overnight at room temperature. After keeping at −20 °C overnight for complete precipitation of *N,N′*-dicyclohexylurea, the by-product was filtered off and the solvent was removed by rotary evaporation.

4.2.3.1. 2,5-Dioxo-1-pyrrolidinyl 2-((2,6-dichlorophenyl)amino) benzeneacetate (12) DFC-NHS. Purification via column chromatography (SiO_2, MeOH/DCM = 1:50) to get **12** as a white solid (yield, 51%). R_f = 0.34 (DCM).

^{1}H NMR (400 MHz, $CDCl_3$): δ 7.35 (d, J = 8.1 Hz, 3H), 7.20 (td, J = 7.8, 1.4 Hz, 1H), 7.06 (td, J = 7.5, 0.9 Hz, 1H), 7.00 (t, J = 8.1 Hz, 1H), 6.64 (d, J = 7.9 Hz, 1H), 6.23 (s, 1H), 4.16 (s, 2H), 2.85 (s, 4H) ppm.

^{13}C{1H} NMR (101 MHz, $CDCl_3$): δ 168.8, 167.3, 142.8, 138.2, 131.1, 129.3, 128.8, 124.1, 123.4, 123.1, 119.9, 34.9, 25.6 ppm.

ESI-MS (positive mode, *m/z*) $[M+H]^+$ calc. for $C_{18}H_{15}O_4N_2Cl_2$: 393.0, found 393.0; *m/z* $[M+Na]^+$ calc. for $C_{18}H_{14}O_4N_2Cl_2Na$: 415.0, found 415.0.

Anal Calc. for $C_{18}H_{14}O_4N_2Cl_2$: C, 54.98; H, 3.59; N, 7.12%. Found: C, 54.71; H, 3.61; N, 6.87%.

4.2.3.2. (2,5-Dioxopyrrolidin-1-yl) 2-hydroxybenzoate (13) SA-NHS. Purification via column chromatography (SiO_2, MeOH/DCM = 1/20) to give **13** as an off-white solid (yield, 69%). R_f = 0.29 (DCM).

^{1}H NMR (400 MHz, $CDCl_3$): δ 9.51 (s, 1H), 8.00 (dd, J = 8.0, 1.6 Hz, 1H), 7.58 (t, J = 7.86 Hz, 1H), 7.05 (d, J = 8.4 Hz, 1H), 6.98 (t, J = 7.6 Hz, 1H), 2.92 (s, 4H).

^{13}C{^{1}H} NMR (101 MHz, $CDCl_3$): δ 168.9, 165.1, 162.2, 137.9, 130.1, 120.0, 118.1, 108.2, 25.7 ppm.

Anal Calc. for $C_{11}H_9NO_5$: C, 56.17; H, 3.86; N, 5.96%. Found: C, 56.33; H, 3.89; N, 5.86%.

4.2.3.3. (2,5-Dioxopyrrolidin-1-yl) 2-((2-hydroxybenzoyl)oxy)benzoate (14) SSA-NHS. Purification via column chromatography (SiO_2, MeOH/DCM = 1/20) to give **14** as a white solid (yield, 72%). R_f = 0.27 (DCM).

^{1}H NMR (400 MHz, $CDCl_3$): δ 10.21 (s, 1H), 8.21 (dd, J = 7.9, 1.5 Hz, 1H), 8.09 (dd, J = 7.9, 1.5 Hz, 1H), 7.74 (t, J = 7.8 Hz, 1H), 7.51 (t, J = 7.8 Hz, 2H), 7.45 (t, J = 7.6 Hz, 2H), 7.35 (d, J = 8.2 Hz, 1H), 7.01 (d, J = 8.2, 1H), 6.95 (t, J = 7.6 Hz, 1H), 2.78 (br s, 4H) ppm.

^{13}C{^{1}H} NMR (101 MHz, $CDCl_3$): δ 168.9, 168.2, 162.2, 159.4, 150.6, 136.6, 135.9, 132.3, 130.8, 126.8, 124.3, 119.6, 119.0, 117.7, 111.6, 25.6 ppm.

Anal Calc. for $C_{18}H_{13}NO_7$: C, 60.85; H, 3.69; N, 3.94%. Found: C, 60.87; H, 3.67; N, 3.87%.

4.2.3.4. (2,5-Dioxopyrrolidin-1-yl) 2′,4′-difluoro-3-hydroxy[1,1′-biphenyl]-4-carboxylate (15) DFS-NHS. Purification via column chromatography (SiO_2, MeOH/DCM = 1/20). Yield: 15%. R_f = 0.30 (DCM).

The single crystal of compound **15** was obtained by slow evaporation of solution in MeOH-DCM (1:20) at room temperature. The molecular structure was determined by using X-ray crystallography (see Table S1 and Fig. S. 76).

^{1}H NMR (400 MHz, $CDCl_3$): δ 9.57 (s, 1H), 8.12 (d, J = 1.8 Hz, 1H), 7.73 (dt, J = 8.8, 1.9 Hz, 1H), 7.41–7.35 (m, 1H), 7.13 (d, J = 8.8 Hz, 1H), 6.98–6.89 (m, 2H), 2.93 (br s, 4H) ppm.

13C{^{1}H} NMR (101 MHz, $CDCl_3$): δ 168.8 (s), 165.0 (s), 163.6 (d, J = 11.8 Hz), 161.7 (s), 161.0 (dd, J = 25.4, 11.8 Hz), 158.4 (d, J = 11.9 Hz), 138.4 (d, J = 3.3 Hz), 131.1 (dd, J = 9.5, 4.6 Hz), 130.1 (d, J = 2.5 Hz), 127.1 (s), 123.4 (dd, J = 13.6, 3.9 Hz), 118.4 (s), 111.8 (dd, J = 21.2, 3.8 Hz), 108.4 (s), 104.5 (t, J = 25.7 Hz), 25.7 (s) ppm.

^{19}F{^{1}H} NMR (376 MHz, $CDCl_3$): δ −113, −116 ppm.

Anal Calc. for $C_{22}H_{16}O_5F_2$: C, 66.33; H, 4.05%. Found: C, 66.13; H, 4.08%.

*4.2.3.5. 2-[(2,5-Dioxo-1-pyrrolidinyl)methoxy]-2-oxoethyl 2-[(2,6-dichlorophenyl)amino]benzeneacetate **(16)**, 2-[(2,5-Dioxo-1-pyrrolidinyl) methoxy]-2-oxoethyl 2-hydroxybenzoate **(17)**, 2-[(2,5-Dioxo-1-pyrrolidinyl)methoxy]-2-oxoethyl 2-((2-hydroxybenzoyl)oxy) benzoate **(18)**, and 2-[(2,5-Dioxo-1-pyrrolidinyl)methoxy]-2-oxoethyl 2′,4′-difluoro-3-hydroxy[1,1′-biphenyl]-4-carboxylate **(19)**.* After drying by rotary evaporation, compounds **16**–**19** were yielded quantitatively and were used for next the steps directly without any purification.

*4.2.4. Synthesis of compound **21***

*4.2.4.1. 6-((tert-butoxycarbonyl) amino) hexanoic acid (L-Boc) **20**.* To a solution of 6-aminohexanoic acid (1.31g, 10 mmol) and triethylamine (2.8 ml, 20 mmol) in acetone-water (1:1, 30 ml), di-*tert*-butyl dicarbonate (2.40 g, 11 mmol) was added and the reaction mixture was stirred for 4 h at room temperature. Then, the solution was concentrated under vacuum and the residual aqueous solution was acidified with 1 M HCl to pH 4–5. The solution was extracted with dichloromethane and the combined organic phase was washed with brine, dried with anhydrous Na_2SO_4. The solvent was removed by rotary evaporation to give the product as a colourless oil. (2.22 g, 96%).

^{1}H NMR (400 MHz, $CDCl_3$): δ 4.59 (s, 1H), 3.09 (s, 2H), 2.33 (t, J = 7.4 Hz, 2H), 1.68–1.59 (m, 2H), 1.53–1.40 (m, 11H), 1.39–1.30 (m, 2H).

^{13}C{^{1}H} NMR (101 MHz, $CDCl_3$): δ 178.9, 156.1, 79.2, 40.3, 33.9, 29.7, 28.4, 26.2, 24.3 ppm.

*4.2.4.2. L-Boc anhydride **21**.* To a solution of L-Boc (462 mg, 2 mmol) in 20 ml of dichloromethane, DCC (247 mg, 1.2 mmol) was added. The solution was stirred overnight at room temperature, then was kept at −20 °C overnight for complete precipitation of *N,N′*-dicyclohexylurea. The by-product was filtered off and the solvent was removed by a rotary evaporator. Quantitatively yielded product was given as a light yellow solid and was used directly for the next steps without any purification.

*4.2.5. General procedure D for the preparation of complexes **22–25 and 31***

Corresponding NHS esters **12**–**15** (0.33 mmol) were added to a suspension of Pt(IV) precursor (0.30 mmol) in 3 ml of anhydrous DMSO. The suspension was heated to 50 °C and kept stirring for 2 days. The insoluble material was removed through centrifugation. Excessive diethyl ether (2 × 40 ml) was added to remove DMSO.

*4.2.5.1. cis,cis,trans-[Pt(NH$_3$)$_2$Cl$_2$(DCF)(OH)] **22**.* The residue was purified by column chromatography (SiO_2, MeOH/DCM = 1:10) to get **22** as a light brown solid (yield, 44%). R_f = 0.15 (MeOH/DCM = 1/10).

^{1}H NMR (400 MHz, DMSO-d_6): δ 7.64 (s, 1H), 7.50 (d, J = 8.1 Hz, 2H), 7.16 (t, J = 7.1 Hz, 2H), 7.03 (t, J = 7.6 Hz, 1H), 6.81 (t, J = 7.3 Hz, 1H), 6.26 (d, J = 7.9 Hz, 1H), 6.17–5.72 (m, 6H), 3.69 (s, 2H) ppm.

^{13}C{^{1}H} NMR (101 MHz, DMSO-d_6): δ 179.7, 143.6, 138.0, 131.4, 130.4, 129.5, 127.4, 126.4, 125.5, 120.8, 116.2, 41.0 ppm.

195 Pt NMR (86 MHz, DMSO-d_6): δ +1045 ppm.

ESI-MS (positive mode, *m/z*) $[M+H]^+$ calc. for $C_{14}H_{18}O_3N_3Cl_4Pt$: 612.0, found 612.0; $[M+Na]^+$ calc. for $C_{14}H_{17}O_3N_3Cl_4PtNa$: 634.0, found 634.0.

Anal Calc. for $C_{14}H_{17}O_3N_3Cl_4Pt$: C, 27.47; H, 2.80; N, 6.86%. Found: C, 27.77; H, 3.05; N, 7.02%.

*4.2.5.2. cis,cis,trans-[Pt(NH$_3$)$_2$Cl$_2$(SA)(OH)] **23**.* The residue was purified by column chromatography (SiO_2, MeOH/DCM = 1/10) to give **23** as a yellow powder (yield, 49%). R_f = 0.20 (MeOH/DCM = 1/5).

^{1}H NMR (400 MHz, DMSO-d_6): δ 11.43 (br s, 1H), 7.77 (dd, J = 8.7, 1.7 Hz, 1H), 7.38 (t, J = 7.7 Hz, 1H), 6.86–6.82 (m, 1H), 6.26–5.87 (m, 6H) ppm.

^{13}C{^{1}H} NMR (101 MHz, DMSO-d_6): δ 175.0, 160.3, 134.2, 131.4, 118.7, 117.5, 116.9 ppm.

195 Pt NMR (100 MHz, DMSO-d_6): δ +1036 ppm.

MS-ESI (negative mode, *m/z*): $[M-H]^-$ Found 452.97, Calc. 453.16; $[M+Cl]^-$ Found 489.95, Calc. 489.62.

Anal Calc. for $C_7H_{12}O_4N_2Cl_2Pt$: C, 18.51; H, 2.66; N, 6.17%. Found: C, 18.89; H, 2.87; N, 6.46%.

*4.2.5.3. cis,cis,trans-[Pt(NH$_3$)$_2$Cl$_2$(SSA)(OH)] **24**.* The residue was purified by column chromatography (SiO_2, MeOH/DCM = 1/10) to give **24** as a yellow powder (yield, 29%). R_f = 0.20 (MeOH/DCM = 1/10).

^{1}H NMR (400 MHz, DMSO-d_6): δ 10.12 (br s, 1H), 8.04 (dd, J = 7.9, 1.6 Hz, 1H), 7.96 (dd, J = 7.8, 1.7 Hz, 1H), 7.60–7.55 (m, 2H), 7.38 (td, J = 7.6, 1.1 Hz, 1H), 7.28 (dd, J = 8.1, 0.9 Hz, 1H), 7.03–6.98 (m, 2H), 6.07–5.75 (m, 6H) ppm.

^{13}C{^{1}H} NMR (101 MHz, DMSO-d_6): δ 172.0, 167.3, 160.4, 149.0, 136.2, 132.8, 132.3, 131.8, 128.3, 126.3, 124.0, 119.9, 117.9, 114.0 ppm.

195 Pt NMR (86 MHz, DMSO-d_6): δ +1036 ppm.

MS-ESI (positive mode, *m/z*): $[M+H]^+$ Found 575.01, Calc. 575.19; $[M+Na]^+$ Found 597.99, Calc. 597.27.

MS-ESI (negative mode, *m/z*): $[M-H]^-$ Found 573.01, Calc. 573.27; $[M+Cl]^-$ Found 609.98, Calc. 609.73.

Anal Calc. for $C_{14}H_{16}O_6N_2Cl_2Pt$: C, 29.28; H, 2.81; N, 4.88%. Found: C, 29.08; H, 3.13; N, 4.74%.

*4.2.5.4. cis,cis,trans-[Pt(NH$_3$)$_2$Cl$_2$(DFS)(OH)] **25**.* The residue was purified by column chromatography (SiO_2, MeOH/DCM = 1/10) to give **25** as a white powder (yield, 42%). R_f = 0.11 (MeOH/DCM = 1/10).

^{1}H NMR (400 MHz, DMSO-d_6): δ 11.63 (s, 1H), 7.93–7.89 (m, 1H), 7.56–7.47 (m, 2H), 7.38–7.31 (m, 1H), 7.18 (td, J = 8.4, 2.1 Hz, 1H), 6.96 (d, J = 8.5 Hz, 1H), 6.31–5.81 (m, 6H) ppm.

^{13}C{^{1}H} NMR (151 MHz, DMSO-d_6): δ 174.6 (s), 162.8 (s), 162.6 (d, J = 12.4 Hz), 161.0 (d, J = 12.2 Hz), 160.2 (d, J = 12.2 Hz), 160.1 (s), 158.6 (d, J = 12.3 Hz), 134.5 (s), 131.9 (dd, J = 9.6, 4.7 Hz), 131.6 (s), 124.8 (d, J = 9.0 Hz), 117.5 (d, J = 8.9 Hz), 116.8 (s), 112.5 (dd, J = 21.0, 3.5 Hz), 105.0 (t, J = 26.6 Hz) ppm.

19F{1H} NMR (376 MHz, DMSO-d_6): δ −112, −114 ppm.

195 Pt NMR (86 MHz, DMSO-d_6): δ +1032 ppm.

MS-ESI (positive mode, *m/z*): $[M+H]^+$ Found 566.00, Calc. 566.00; $[M+Na]^+$ Found 587.98, Calc. 587.98.

MS-ESI (negative mode, *m/z*): $[M-H]^-$ Found 563.99, Calc. 563.98.

Anal Calc. for $C_{13}H_{14}O_4N_2F_2Cl_2Pt$: C, 27.57; H, 2.49; N, 4.95%. Found: C, 27.44; H, 2.54; N, 4.90%.

*4.2.5.5. [Pt(DACH)(DCF)(OH)ox] **31**.* The residue was purified by column chromatography (SiO_2, MeOH/DCM = 1:10) to get **31** as a white solid (yield, 45%). R_f = 0.16 (MeOH/DCM = 1/10).

^{1}H NMR (400 MHz, DMSO-d_6): δ 8.39–7.68 (m, 7H), 7.60–7.46 (m, 6H), 7.17 (t, J = 8.2 Hz, 4H), 7.04 (t, J = 7.7 Hz, 2H), 6.82 (t, J = 7.4 Hz, 2H), 6.28 (d, J = 8.0 Hz, 2H), 3.72 (s, 4H), 2.67–2.59 (m, 4H), 2.08–1.95 (m, 4H), 1.53–1.40 (m, 6H), 1.30–1.24 (m, 2H), 1.13–0.94 (m, 4H) ppm.

^{13}C{^{1}H} NMR (101 MHz, DMSO-d_6): δ 180.8, 164.3, 143.2, 137.7, 131.3, 130.0, 129.7, 127.6, 125.9, 125.6, 121.1, 116.4, 61.6, 60.6, 41.1, 31.2, 24.2 ppm.

195 Pt NMR (86 MHz, DMSO-d_6): δ +1410 ppm.

ESI-MS (positive mode, *m/z*) $[M+H]^+$ calc. for $C_{22}H_{26}O_7N_3Cl_2Pt$: 710.1, found 710.1; $[M+Na]^+$ calc. for $C_{22}H_{25}O_7N_3Cl_2PtNa$: 732.1, found 732.1.

ESI-MS (negative mode, *m/z*) $[M-H]^-$ calc. for $C_{22}H_{24}O_7N_3Cl_2Pt$: 708.1, found 708.1.

Anal Calc. for $C_{22}H_{25}O_7N_3Cl_2Pt$: C, 37.25; H, 3.55; N, 5.92%. Found: C, 37.12; H, 3.73; N, 5.75%.

*4.2.6. General procedure E for the preparation of **26–29***

The corresponding NHS esters **16**–**19** (0.50 mmol) were added to a suspension of oxoplatin (0.20 mmol) in 4 ml of anhydrous DMSO. The

suspension was heated to 50 °C and kept stirring overnight. The insoluble material was removed through centrifugation. Excessive diethyl ether (2 × 20 ml) was added to remove DMSO.

*4.2.6.1. cis,cis,trans-[Pt(NH$_3$)$_2$Cl$_2$(ACF)$_2$] **26**.* The residue was purified by column chromatography (SiO_2, MeOH/DCM = 1:50) to get **26** as a light brown solid (yield, 46%). R_f = 0.39 (MeOH/DCM = 1/20).

^{1}H NMR (400 MHz, DMSO-d_6): δ 7.53 (d, J = 8.1 Hz, 2H), 7.26 (dd, J = 7.5, 1.2 Hz, 1H), 7.21 (t, J = 8.1 Hz, 1H), 7.11–7.04 (m, 1H), 6.96 (s, 1H), 6.92–6.85 (m, 1H), 6.52 (s, 3H), 6.28 (d, J = 7.9 Hz, 1H), 4.67 (s, 2H), 3.87 (s, 2H) ppm.

^{13}C{^{1}H} NMR (101 MHz, DMSO-d_6): δ 174.9, 171.3, 143.4, 137.7, 131.5, 131.1, 129.6, 128.3, 126.3, 123.9, 121.4, 116.8, 60.9, 37.4 ppm.

195 Pt NMR (86 MHz, DMSO-d_6): δ +1239 ppm.

ESI-MS (positive mode, m/z) $[M+H]^+$ calc. for $C_{32}H_{31}O_8N_4Cl_6Pt$: 1007.4, found 1007.0.

Anal Calc. for $C_{32}H_{30}O_8N_4Cl_6Pt$: C, 38.19; H, 3.00; N, 5.57%. Found: C, 38.32; H, 2.93; N, 5.38%.

*4.2.6.2. cis,cis,trans-Pt[(NH$_3$)$_2$Cl$_2$(ASA)$_2$] **27**.* The residue was purified by column chromatography (SiO_2, MeOH/DCM = 1:40) to get **27** as a light brown solid (yield, 40%). R_f = 0.29 (MeOH/DCM = 1/20).

^{1}H NMR (400 MHz, DMSO-d_6): δ 10.32 (s, 2H), 7.87–7.81 (m, 2H), 7.58–7.53 (m, 2H), 7.04–6.96 (m, 4H), 6.55 (s, 6H), 4.91 (s, 4H) ppm.

13C{1H} NMR (101 MHz, DMSO-d_6): δ 175, 168, 160, 136, 131, 120, 118, 113, 61 ppm.

195 Pt NMR (86 MHz, DMSO-d_6): δ +1238 ppm.

ESI-MS (positive mode, m/z) $[M-H]^-$ calc. for $C_{18}H_{19}O_{10}N_2Cl_2Pt$: 689.3, found 689.0.

Anal Calc. for $C_{18}H_{20}O_{10}N_2Cl_2Pt$: C, 31.32; H, 2.92; N, 4.06%. Found: C, 31.65; H, 3.14; N, 3.97%.

*4.2.6.3. cis,cis,trans-Pt[(NH$_3$)$_2$Cl$_2$(ASSA)$_2$] **28**.* The residue was purified by column chromatography (SiO_2, MeOH/DCM = 1:80) to get **28** as a light brown solid (yield, 9%). R_f = 0.13 (MeOH/DCM = 1/40).

^{1}H NMR (300 MHz, $CDCl_3$): δ 10.24 (s, 2H), 8.08 (t, J = 7.8 Hz, 4H), 7.63 (t, J = 7.6 Hz, 2H), 7.48 (t, J = 7.3 Hz, 2H), 7.37 (t, J = 7.6 Hz, 2H), 7.24 (d, J = 8.0 Hz, 2H), 6.97 (dd, J = 7.8, 6.0 Hz, 4H), 5.44 (s, 6H), 4.68 (s, 4H) ppm.

13C{1H} NMR (101 MHz, CD2Cl2): δ 177, 169, 165, 161, 150, 137, 135, 132, 131, 127, 124, 123, 120, 118, 112, 62 ppm.

195 Pt NMR (86 MHz, CD_2Cl_2): δ +1087 ppm.

ESI-MS (positive mode, m/z) $[M+H]^+$ calc. for $C_{32}H_{29}O_{14}N_2Cl_2Pt$: 931.5, found 931.1; $[M+Na]^+$ calc. for $C_{32}H_{29}O_{14}N_2Cl_2PtNa$: 953.5, found 953.1.

Anal Calc. for $C_{32}H_{28}O_{14}N_2Cl_2Pt$: C, 41.30; H, 3.03; N, 3.01%. Found: C, 41.61; H, 3.16; N, 2.97%.

*4.2.6.4. cis,cis,trans-Pt[(NH$_3$)$_2$Cl$_2$(ADFS)$_2$] **29**.* The residue was purified by column chromatography (SiO_2, MeOH/DCM = 1:80) to get **29** as a yellowish solid (yield, 40%). R_f = 0.10 (MeOH/DCM = 1/40).

^{1}H NMR (400 MHz, DMSO-d_6): δ 10.42 (s, 1H), 7.96 (s, 1H), 7.71 (dd, J = 8.7, 1.5 Hz, 1H), 7.57 (dd, J = 8.9, 2.2 Hz, 1H), 7.39–7.33 (m, 1H), 7.21–7.16 (m, 1H), 7.13 (d, J = 8.6 Hz, 1H), 6.55 (s, 3H), 4.92 (s, 2H) ppm.

^{13}C{^{1}H} NMR (101 MHz, DMSO-d_6): δ 174.5 (s), 167.5 (s), 163.3 (d, J = 12.2 Hz), 160.7 (t, J = 11.6 Hz), 159.9 (s), 158.3 (d, J = 12.3 Hz), 136.4 (s), 132.0 (dd, J = 9.7, 4.6 Hz), 130.8 (s), 125.8 (s), 124.0 (dd, J = 13.3, 3.8 Hz), 118.5 (s), 113.9 (s), 112.6 (dd, J = 21.2, 3.6 Hz), 105.0 (t, J = 26.4 Hz), 61.2 (s) ppm.

^{195}Pt NMR (86 MHz, DMSO-d_6): δ +1234 ppm.

19F{1H} NMR (282 MHz, DMSO-d_6): δ −111, −113 ppm.

ESI-MS (negative mode, m/z) $[M-H]^-$ calc. for $C_{30}H_{23}O_{10}N_2Cl_2F_4Pt$: 913.5, found 913.0.

Anal Calc. for $C_{30}H_{24}O_{10}N_2Cl_2F_4Pt$: C, 39.40; H, 2.65; N, 3.06%. Found: C, 39.68; H, 2.90; N, 2.93%.

*4.2.7. Synthesis of cis,cis,trans-[Pt(NH$_3$)$_2$Cl$_2$(DCF)(OAc)] **30***

Acetic anhydride (53 mg, 0.52 mmol) was added to a solution of complex **22** (53 mg, 0.086 mmol) in 4 ml of dry DMF. The solution was stirred overnight at room temperature. Then DMF was removed by rotary evaporation and the obtained residue was purified by column chromatography (SiO_2, MeOH/DCM = 1:30) to get a light brown solid (55 mg, 46%). R_f = 0.21 (MeOH/DCM = 1/20).

^{1}H NMR (300 MHz, DMSO-d_6): δ 7.49 (d, J = 8.1 Hz, 2H), 7.25 (s, 1H), 7.19–7.11 (m, 2H), 7.02 (t, J = 7.5 Hz, 1H), 6.81 (t, J = 6.6 Hz, 1H), 6.41 (br s, 6H), 6.24 (d, J = 8.0 Hz, 1H), 3.75 (s, 2H), 1.91 (s, 3H).

^{13}C{^{1}H} NMR (101 MHz, DMSO-d_6) δ 179.3, 178.8, 143.6, 137.9, 131.4, 130.8, 129.5, 127.6, 125.8, 125.7, 120.8, 116.1, 40.9, 23.4 ppm.

195 Pt NMR (86 MHz, DMSO-d_6): δ +1229 ppm.

ESI-MS (positive mode, m/z) $[M+H]^+$ calc. for $C_{16}H_{20}O_4N_3Cl_4Pt$: 654.0, found 654.0; $[M+Na]^+$ calc. for $C_{16}H_{19}O_4N_3Cl_4PtNa$: 676.0, found 676.0.

Anal Calc. for $C_{16}H_{19}O_4N_3Cl_4Pt$: C, 29.37; H, 2.93; N, 6.42%. Found: C, 29.48; H, 3.10; N, 6.24%.

*4.2.8. Synthesis of [Pt(DACH)(DCF)(OAc)ox] **32***

Following the same procedure of preparation for **30**, complex **32** was synthesized from 20 mg of complex **31**. The residue was purified by column chromatography (SiO_2, MeOH/DCM = 1:20), obtaining **32** as a white solid (16 mg, 76%). R_f = 0.13 (MeOH/DCM = 1/20).

^{1}H NMR (400 MHz, DMSO-d_6): δ 8.52–8.20 (m, 3H), 8.12–7.93 (m, 1H), 7.52 (d, J = 8.1 Hz, 2H), 7.25 (s, 1H), 7.18 (t, J = 8.1 Hz, 2H), 7.09–7.02 (m, 1H), 6.83 (t, J = 7.1 Hz, 1H), 6.28 (d, J = 7.9 Hz, 1H), 3.78 (s, 2H), 2.69–2.53 (m, 2H), 2.14–2.04 (m, 2H), 1.97 (s, 3H), 1.52–1.32 (m, 4H), 1.18–0.99 (m, 2H) ppm.

^{13}C{^{1}H} NMR (101 MHz, DMSO-d_6): δ 179.6, 178.8, 163.9, 143.2, 137.6, 131.4, 130.2, 129.6, 127.8, 125.8, 125.2, 121.2, 116.4, 61.6, 61.3, 31.4, 24.0, 23.9, 23.4 ppm.

195 Pt NMR (86 MHz, DMSO-d_6): +1575 ppm.

ESI-MS (positive mode, m/z) $[M+H]^+$ calc. for $C_{24}H_{28}O_8N_3Cl_2Pt$: 752.1, found 752.1.

ESI-MS (negative mode, m/z) $[M-H]^-$ calc. for $C_{24}H_{26}O_8N_3Cl_2Pt$: 750.1, found 750.1.

Anal Calc. for $C_{24}H_{27}O_8N_3Cl_2Pt$: C, 38.36; H, 3.62; N, 5.59%. Found: C, 37.99; H, 3.69; N, 5.48%.

*4.2.9. Synthesis of [Pt(DACH)(L-Boc)$_2$ox] **33***

L-Boc anhydride (391 mg, 1.2 mmol) was added to a suspension of dihydroxido oxaliplatin(IV) (95 mg, 0.22 mmol) in 5 ml of DMF. The mixture was stirred for 4 days at room temperature. Then DMF was removed by rotary evaporation and the obtained residue was purified by column chromatography (SiO_2, MeOH/DCM = 1:20) to get a white solid (80 mg, 42%).

^{1}H NMR (400 MHz, DMSO-d_6): δ 8.37 (br s, 4H), 6.75 (t, J = 5.5 Hz, 2H), 2.86 (dd, J = 13.1, 6.7 Hz, 4H), 2.58–2.52 (m, 2H), 2.26–2.22 (m, 4H), 2.12 (d, J = 11.7 Hz, 2H), 1.51–1.30 (m, 30H), 1.22–1.09 (m, 6H).

^{13}C{^{1}H} NMR (101 MHz, DMSO-d_6): δ 181.5, 163.8, 156.0, 77.8, 61.6, 36.2, 31.4, 29.6, 28.7, 26.2, 25.5, 24.0 ppm.

195 Pt NMR (86 MHz, DMSO-d_6): δ +1604 ppm.

ESI-MS (positive mode, m/z) $[M+H]^+$ calc. for $C_{30}H_{55}O_{12}N_4Pt$: 858.3, found 858.3; $[M+Na]^+$ calc. for $C_{30}H_{54}O_{12}N_4PtNa$: 880.3, found 880.3.

Anal Calc. for $C_{30}H_{54}O_{12}N_4Pt$: C, 42.00; H, 6.34; N, 6.53%. Found: C, 42.30; H, 6.38; N, 6.54%.

*4.2.10. Synthesis of [Pt(DACH)(L-DCF)$_2$ox] **34***

Complex **33** (80 mg, 0.093 mmol) was dissolved in 2 ml of DCM, followed by excessive addition of trifluoracetic acid (about 1 ml). The solution was kept stirring for 3 h, then it was dried under reduced pressure. The product was yielded quantitatively and was used for the

next step directly without any purification. Triethylamine (188 mg, 1.86 mmol) and DCF-NHS (110 mg, 0.28 mmol) were added to a solution of product yielded in the prior step in 3 ml of DMF. The solution was stirred overnight at room temperature. Then DMF was removed by rotary evaporation and the obtained residue was purified by column chromatography (SiO_2, MeOH/DCM = 1:20) to get a white solid (70 mg, 62%). R_f = 0.24 (MeOH/DCM = 1/20).

^{1}H NMR (400 MHz, DMSO-d_6): δ 8.44–8.30 (m, 3H), 7.51 (d, J = 8.1 Hz, 2H), 7.26–7.12 (m, 2H), 7.03 (t, J = 7.2 Hz, 1H), 6.85 (t, J = 7.3 Hz, 1H), 6.28 (d, J = 7.9 Hz, 1H), 3.56 (s, 2H), 3.12–2.94 (m, 2H), 2.59–2.52 (m, 1H), 2.31–2.16 (m, 2H), 2.11 (d, J = 10.9 Hz, 1H), 1.53–1.05 (m, 9H) ppm.

^{13}C{^{1}H} NMR (101 MHz, DMSO-d_6): δ 181.4, 171.9, 163.9, 143.4, 137.6, 130.8, 129.8, 129.7, 127.6, 126.0, 125.5, 121.1, 116.4, 61.6, 39.1, 36.2, 31.4, 29.1, 26.3, 25.5, 24.0 ppm.

195 Pt NMR (86 MHz, DMSO-d_6): δ +1604 ppm.

ESI-MS (positive mode, m/z) [M+H]+ calc. for C48H57O10N6Cl4Pt: 1215.3, found 1215.3.

Anal Calc. for $C_{48}H_{56}O_{10}N_6Cl_4Pt$: C, 47.49; H, 4.65; N, 6.92%. Found: C, 47.42; H, 4.66; N, 6.80%.

4.3. Cytotoxicity assay

Subconfluent SW480 (colon carcinoma), CH1/PA-1 (ovarian teratocarcinoma) and A549 (non-small cell lung cancer) cells were harvested by trypsinization for 3–5 min. Supplemented MEM was added to stop trypsinization, and cells were centrifuged for 3 min at 1200 rpm (Thermo Scientific, Megafuge 1.0R). After aspiration of the supernatant, the cell pellet was resuspended in supplemented MEM. Afterwards, CH1/PA-1, SW480, A549 cells were seeded in 100 μL aliquots in densities of 1.0 × 10^3, 2.0 × 10^3 and 3.0 × 10^3 cells/well, respectively, in clear flat-bottom 96-well microculture plates. After incubation of the plates for 24 h, test compounds as well as the reference compounds cisplatin and oxaliplatin were dissolved in 100% DMF, serially diluted in supplemented MEM and added in triplicates of 100 μL/well, whereupon the concentration of DMF did not exceed 0.5% v/v. Plates were incubated for 96 h, then the medium was replaced with 100 μL/well of an MTT-medium mixture (MTT = 3-(4,5-dimethylthiazol-2-yl)-2,5-diphenyltetrazolium bromide). For this purpose, MTT powder had been dissolved in PBS to a concentration of 5 mg/ml and then diluted 1:7 in supplemented RPMI 1640 medium (supplemented with 10% heat-inactivated FBS and 4 mM L-glutamine). After 4 h of incubation, the dyeing solution was replaced with 150 μL/well of DMSO and optical densities were measured at 550 nm (with 690 nm as reference) with a microplate reader (BioTek, ELx808). Interpolated IC_{50} values were averaged from at least three independent experiments. In addition, a single neutral red assay experiment with four compounds (**22**, **26**, **30** and **32**) in CH1/PA-1 cells was performed as described previously [54].

4.4. COX inhibition and analysis of prostaglandins

A549 cells (1 × 10^6) were seeded into 6-well-plates in RPMI 1640 (Thermo Fisher Scientific, Schwerte, Germany) containing heat-inactivated FCS (10% v/v), penicillin (100 U/mL), streptomycin (100 μg/mL) and L-glutamine (2 mmol/L). After attachment, the cells were preincubated with 2 ng/mL IL-1β for 24 h. Then, the supernatant was removed and cells were treated with either DMSO (0.1%), cisplatin, platinum(IV) complexes with ACF, ASSA or ADFS or the free drugs for 15 min in PBS containing 1 mM $CaCl_2$ at 37 °C. Afterwards, cells were treated with 2.5 μM Ca^{2+}-ionophore A23187 (Cayman Chemical/Biomol GmbH, Hamburg, Germany) to induce COX product formation for 10 min at 37 °C. Afterwards, the reaction was stopped by adding 2 mL of ice-cold methanol containing deuterated LM standards (200 nM d8-5S-HETE, d4-LTB_4, d5-LXA_4, d5-RvD2, d4-PGE_2 and 10 μM d8-AA; Cayman Chemical/Biomol GmbH). Then, samples were stored at −20 °C for at least 60 min to allow protein precipitation. The extraction of prostaglandins was performed as recently published [55]. In brief, after centrifugation (1200×*g*; 4 °C; 10 min) acidified H_2O (9 mL; final pH = 3.5) was added and samples were extracted on solid phase cartridges (Sep-Pak® Vac 6 cc 500 mg/6 mL C18; Waters, Milford, MA, USA). Samples were loaded after equilibration with methanol followed by H_2O. After washing with H_2O and *n*-hexane, samples were eluted with methyl formate (6 mL). The solvent was fully evaporated using an evaporation system (TurboVap LV, Biotage, Uppsala, Sweden) and resuspended in 150 μL methanol/water (1:1, v/v) for UPLC-MS-MS analysis. The prostaglandins were analyzed with an Acquity™ UPLC system (Waters, Milford, MA, USA) and a QTRAP 5500 Mass Spectrometer (ABSciex, Darmstadt, Germany) equipped with a Turbo V™ Source and electrospray ionization. Prostaglandins were eluted using an ACQUITY UPLC® BEH C18 column (1.7 μm, 2.1 mm × 100 mm; Waters, Eschborn, Germany) heated at 50 °C with a flow rate of 0.3 mL/min and a mobile phase consisting of methanol-water-acetic acid in the ratio of 42:58:0.01 (v/v/v) that was ramped to 86:14:0.01 (v/v/v) over 12.5 min and then to 98:2:0.01 (v/v/v) for 3 min. The QTRAP 5500 was run in negative ionization mode using scheduled multiple reaction monitoring (MRM) coupled with information-dependent acquisition. The scheduled MRM window was 60 s, optimized prostaglandin parameters were adopted, with a curtain gas pressure of 35 psi. The retention time and at least six diagnostic ions for each prostaglandin were confirmed by means of an external standard (Cayman Chemical/Biomol GmbH, Hamburg, Germany). Quantification was achieved by calibration curves for each prostaglandin. Linear calibration curves were obtained for each prostaglandin and gave r^2 values of 0.998 or higher. Additionally, the limit of detection for each targeted prostaglandin was determined [56].

4.5. Stability study

ACF (1.8 mg) and complex **26** (2.5 mg) were dissolved in a mixture of DMF-d_7 (0.4 ml) and PBS (D_2O, 0.1 ml), respectively. The solution was incubated at 37 °C. The ^{1}H NMR spectra were checked at 0 h and 48 h.

4.6. Reduction study

Complex **26** (2.5 mg) and ascorbic acid (4.4 mg, 10 eq) were incubated in 0.5 ml of DMF-PBS (v/v; 4/1) at 37 °C. The ^{195}Pt NMR spectra were measured after 18 h.

4.7. 9-Methylguanine binding experiment

The mixture of complex **26** (1.3 mg), ascorbic acid (2.3 mg, 10 eq) and 9-methylguanine (0.7 mg, 3 eq) was incubated in 0.5 ml of DMF-PBS (v/v; 4/1) at 37 °C. After 24 h, the reaction solution was checked by LC-ESI-MS.

4.8. Cellular accumulation

Subconfluent SW480 cells were harvested by trypsinization for 4–5 min. Supplemented MEM was added to stop trypsinization, and cells were centrifuged for 3 min at 1200 rpm. After aspiration of the supernatant, the cell pellet was resuspended in supplemented MEM. Then, cells were seeded in 1 mL triplicates in a density of 1.5 × 10^5 cells/well in clear flat-bottom 12-well microculture plates and incubated for 24 h. Afterwards, medium was aspirated and 50 μM (prepared from 100% DMF stock solution) of each test compound in supplemented MEM (500 μL/well) were applied for 2 h. Medium was aspirated and cells were washed 3 × with PBS. 400 μL/well nitric acid were added for 1 h at room temperature, then 300 μL of acidified suspension were transferred into 7.7 mL MilliQ water in 15 mL tubes. Pt concentrations (ng/mL) were quantified by ICP-MS as described previously.[29] Note: To enable assessments of Pt amounts in fg/cell, a reference plate for cell counting was seeded simultaneously with the test plates. After incubation for 24 h, cells were washed 3 × with PBS and trypsinized for 5 min (500 μL/well). Single-cell suspensions were

transferred into 1.5 mL tubes and filled to 1 ml with PBS. Cells were counted by using a hemocytometer and the mean of three counts was taken for calculation of cellular Pt contents.

4.9. JC-1 assay

Changes in cells' mitochondrial membrane potential were quantitatively analyzed via flow cytometry using the polychromatic JC-1 dye (2 mg, final 5 mM DMSO solution, *MCE*), which emits orange fluorescence in intact mitochondria, but green fluorescence in damaged ones. For these experiments, SW480 cells were seeded into 48-well plates (7×10^4 cells/well) in 600 μL aliquots of MEM and allowed to settle for 24 h. Afterwards, cells were incubated with different concentrations (prepared from 100% DMF stock solutions) of compounds **24** and **26** for 24 h. After treatment, the supernatant was removed and cells were washed once with PBS. The washing solution was collected and cells were trypsinized for 5 min at 37 °C. Trypsinization was stopped by adding supplemented MEM, the resulting cell suspension was added to the pre-collected medium and cells were centrifuged (300 g, 3 min). Then, the supernatant was removed and the cell pellet was resuspended with 500 μL JC-1/MEM solution (200 μM DMSO stock, final concentration: 2 μM) and incubated for 15 min at 37 °C. Cells were centrifuged and the supernatant was discarded. Before analysis with a Millipore Guava easyCyte 8HT instrument with InCyte software, the cell pellet was resuspended in 250 μL PBS. At least three independent experiments were quantified by FlowJo software.

4.10. Apoptosis/necrosis assay

Apoptosis was quantitatively analyzed by flow cytometry using double staining with FITC-conjugated annexin V (eBioscience) and propidium iodide (PI, 1.0 mg/mL, Sigma-Aldrich). SW480 cells were seeded into 48-well plates (7×10^4 cells/well) in 600 μL MEM per well and allowed to settle for 24 h. Afterwards, cells were incubated with different concentrations (prepared from 100% DMF stock solutions) of compounds **24** and **26** for 24 h. After treatment, the supernatant was removed and cells were washed once with PBS. The washing solution was collected and cells were trypsinized for 5 min at 37 °C. Trypsinization was stopped by adding supplemented MEM, the resulting cell suspension was added to the pre-collected medium and cells were centrifuged (300 g, 3 min). Then, the supernatant was removed and the cell pellet was resuspended with 1.5 μL FITC-conjugated annexin V in 150 μL binding buffer (10 mM HEPES/NaOH pH 7.4, 140 mM NaCl and 2.5 mM $CaCl_2 \bullet 2H_2O$) and incubated for 15 min at 37 °C. 1 μL of propidium iodide in 150 μL binding buffer was added shortly before flow-cytometric analysis, using a Millipore Guava easyCyte 8HT instrument with InCyte software. Results of at least three independent experiments were evaluated by using FlowJo software.

Disclaimer

The authors declare no conflict of interest.

Declaration of competing interest

The authors declare that they have no known competing financial interests or personal relationships that could have appeared to influence the work reported in this paper.

Data availability

Data will be made available on request.

Acknowledgment

This research was funded by a grant from China Scholarship Council (CSC) and by the Deutsche Forschungsgemeinschaft SFB1278/2 Polytarget (project no. 316213987). We thank Umicore AG & Co. KG Hanau-Wolfgang for the generous loan of potassium tetrachloroplatinate(II) compound. We are grateful for the suggestion provided by Dr. Nico Überschaar for the characterization of the targeted compounds.

Appendix A. Supplementary data

Supplementary data to this article can be found online at https://doi.org/10.1016/j.ejmech.2023.115515.

References

[1] S.I. Grivennikov, F.R. Greten, M. Karin, Immunity, inflammation, and cancer, Cell 140 (2010) 883–899, https://doi.org/10.1016/j.cell.2010.01.025.
[2] M. Murata, Inflammation and cancer, Environ Health Prev 23 (2018) 50, https://doi.org/10.1186/s12199-018-0740-1.
[3] F.R. Greten, S.I. Grivennikov, Inflammation and cancer: triggers, mechanisms, and consequences, Immunity 51 (2019) 27–41, https://doi.org/10.1016/j.immuni.2019.06.025.
[4] H.K. Zhao, L. Wu, G.F. Yan, Y. Chen, M.Y. Zhou, Y.Z. Wu, Y.S. Li, Inflammation and tumor progression: signaling pathways and targeted intervention, Signal Transduct Tar 6 (2021) 263, https://doi.org/10.1038/s41392-021-00658-5.
[5] P. Pęczek, M. Gajda, K. Rutkowski, M. Fudalej, A. Deptała, A.M. Badowska-Kozakiewicz, Cancer-associated inflammation: pathophysiology and clinical significance, J Cancer Res Clin 149 (2023) 2657–2672, https://doi.org/10.1007/s00432-022-04399-y.
[6] A. Greenhough, H.J. Smartt, A.E. Moore, H.R. Roberts, A.C. Williams, C. Paraskeva, A. Kaidi, The COX-2/PGE2 pathway: key roles in the hallmarks of cancer and adaptation to the tumour microenvironment, Carcinogenesis 30 (2009) 377–386, https://doi.org/10.1093/carcin/bgp014.
[7] B. Liu, L.Y. Qu, S.G. Yan, Cyclooxygenase-2 promotes tumor growth and suppresses tumor immunity, Cancer Cell Int. 15 (2015) 106, https://doi.org/10.1186/s12935-015-0260-7.
[8] L.Y. Pang, E.A. Hurst, D.J. Argyle, Cyclooxygenase-2: a role in cancer stem cell survival and repopulation of cancer cells during therapy, Stem Cell. Int. (2016), 2048731, https://doi.org/10.1155/2016/2048731, 2016.
[9] V. Karpisheh, A. Nikkhoo, M. Hojjat-Farsangi, A. Namdar, G. Azizi, G. Ghalamfarsa, G. Sabz, M. Yousefi, B. Yousefi, F. Jadidi-Niaragh, Prostaglandin E2 as a potent therapeutic target for treatment of colon cancer, Prostag. Other Lipid Mediat. 144 (2019), 106338, https://doi.org/10.1016/j.prostaglandins.2019.106338.
[10] F. Finetti, C. Travelli, J. Ercoli, G. Colombo, E. Buoso, L. Trabalzini, Prostaglandin E2 and cancer: insight into tumor progression and immunity, Bio-Basel 9 (2020) 434, https://doi.org/10.3390/biology9120434.
[11] Y. Zhang, S. Tighe, Y.T. Zhu, COX-2 signaling in the tumor microenvironment, Adv. Exp. Med. Biol. 1277 (2020) 87–104, https://doi.org/10.1007/978-3-030-50224-9_6.
[12] N.U. Mohsin, S. Aslam, M. Ahmad, M. Irfan, S.A. Al-Hussain, M.E.A. Zaki, Cyclooxygenase-2 (COX-2) as a target of anticancer agents: a review of novel synthesized scaffolds having anticancer and COX-2 inhibitory potentialities, Pharmaceut. Biol. 15 (2022) 1471, https://doi.org/10.3390/ph15121471.
[13] R.S.Y. Wong, Role of nonsteroidal anti-inflammatory drugs (NSAIDs) in cancer prevention and cancer promotion, Adv Pharmacol Sci (2019), 3418975, https://doi.org/10.1155/2019/3418975, 2019.
[14] S. Zappavigna, A.M. Cossu, A. Grimaldi, M. Bocchetti, G.A. Ferraro, G.F. Nicoletti, R. Filosa, M. Caraglia, Anti-inflammatory drugs as anticancer agents, Int. J. Mol. Sci. 21 (2020) 2605, https://doi.org/10.3390/ijms21072605.
[15] S. Ramos-Inza, A.C. Ruberte, C. SanmartÍn, A.K. Sharma, D. Plano, NSAIDs: old acquaintance in the pipeline for cancer treatment and prevention-structural modulation, mechanisms of action, and bright future, J. Med. Chem. 64 (2021) 16380–16421, https://doi.org/10.1021/acs.jmedchem.1c01460.
[16] T.C. Johnstone, K. Suntharalingam, S.J. Lippard, The next generation of platinum drugs: targeted Pt(II) agents, nanoparticle delivery, and Pt(IV) prodrugs, Chem. Rev. 116 (2016) 3436–3486, https://doi.org/10.1021/acs.chemrev.5b00597.
[17] R.G. Kenny, S.W. Chuah, A. Crawford, C.J. Marmion, Platinum(IV) prodrugs - a step closer to ehrlich's vision? Eur. J. Inorg. Chem. (2017) 1596–1612, https://doi.org/10.1002/ejic.201601278.
[18] D. Gibson, Pt(IV) anticancer prodrugs - a tale of mice and men, ChemMedChem 16 (2021) 2188–2191, https://doi.org/10.1002/cmdc.202100115.
[19] Z.F. Xu, Z.G. Wang, Z.Q. Deng, G.Y. Zhu, Recent advances in the synthesis, stability, and activation of platinum (IV) anticancer prodrugs, Coord. Chem. Rev. 442 (2021), 213991, https://doi.org/10.1016/j.ccr.2021.213991.
[20] M. Ravera, E. Gabano, M.J. McGlinchey, D. Osella, Pt(iv) antitumor prodrugs: dogmas, paradigms, and realities, Dalton Trans. 51 (2022) 2121–2134, https://doi.org/10.1039/D1DT03886A.
[21] D. Gibson, Platinum(IV) anticancer agents; are we en route to the holy grail or to a dead end? J. Inorg. Biochem. 217 (2021), 111353 https://doi.org/10.1016/j.jinorgbio.2020.111353.
[22] L. Larasati, W.W. Lestari, M. Firdaus, Dual-action Pt(IV) prodrugs and targeted delivery in metal-organic frameworks: overcoming cisplatin resistance and improving anticancer activity, Bull. Chem. Soc. Jpn. 95 (2022) 1561–1577, https://doi.org/10.1246/bcsj.20220218.

[23] W. Neumann, B.C. Crews, M.B. Sárosi, C.M. Daniel, K. Ghebreselasie, M.S. Scholz, L.J. Marnett, E. Hey-Hawkins, Conjugation of cisplatin analogues and cyclooxygenase inhibitors to overcome cisplatin resistance, ChemMedChem 10 (2015) 183–192, https://doi.org/10.1002/cmdc.201402353.
[24] A. Curci, N. Denora, R.M. Iacobazzi, N. Ditaranto, J.D. Hoeschele, N. Margiotta, G. Natile, Synthesis, characterization, and in vitro cytotoxicity of a Kiteplatin-Ibuprofen Pt(IV) prodrug, Inorg. Chim. Acta. 472 (2018) 221–228, https://doi.org/10.1016/j.ica.2017.07.019.
[25] X.Q. Song, Z.Y. Ma, Y.G. Wu, M.L. Dai, D.B. Wang, J.Y. Xu, Y.Z. Liu, New NSAID-Pt (IV) prodrugs to suppress metastasis and invasion of tumor cells and enhance anti-tumor effect in vitro and in vivo, Eur. J. Med. Chem. 167 (2019) 377–387, https://doi.org/10.1016/j.ejmech.2019.02.041.
[26] S.X. Jin, N. Muhammad, Y.W. Sun, Y.H. Tan, H. Yuan, D.F. Song, Z.J. Guo, X. Y. Wang, Multispecific platinum(IV) complex deters breast cancer via interposing inflammation and immunosuppression as an inhibitor of COX-2 and PD-L1, Angew. Chem., Int. Ed. 59 (2020) 23313–23321, https://doi.org/10.1002/anie.202011273.
[27] D. Spector, O. Krasnovskaya, K. Pavlov, A. Erofeev, P. Gorelkin, E. Beloglazkina, A. Majouga, Pt(IV) prodrugs with NSAIDs as axial ligands, Int. J. Mol. Sci. 22 (2021) 3817, https://doi.org/10.3390/ijms22083817.
[28] D.V. Spector, K.G. Pavlov, R.A. Akasov, A.N. Vaneev, A.S. Erofeev, P.V. Gorelkin, V.N. Nikitina, E.V. Lopatukhina, A.S. Semkina, K.Y. Vlasova, D.A. Skvortsov, V. A. Roznyatovsky, N.V. Ul'yanovskiy, I.I. Pikovskoi, S.A. Sypalov, A.S. Garanina, S. S. Vodopyanov, M.A. Abakumov, Y.L. Volodina, A.A. Markova, A.S. Petrova, D. M. Mazur, D.A. Sakharov, N.V. Zyk, E.K. Beloglazkina, A.G. Majouga, O. O. Krasnovskaya, Pt(IV) prodrugs with non-steroidal anti-inflammatory drugs in the axial position, J. Med. Chem. 65 (2022) 8227–8244, https://doi.org/10.1021/acs.jmedchem.1c02136.
[29] I. Predarska, M. Saoud, I. Morgan, T. Eichhorn, G.N. Kaluderovic, E. Hey-Hawkins, Cisplatin-cyclooxygenase inhibitor conjugates, free and immobilised in mesoporous silica SBA-15, prove highly potent against triple-negative MDA-MB-468 breast cancer cell line, Dalton Trans. 51 (2022) 857–869, https://doi.org/10.1039/D1DT03265H.
[30] A. Khoury, J.A. Sakoff, J. Gilbert, K.F. Scott, S. Karan, C.P. Gordon, J.R. Aldrich-Wright, Cyclooxygenase-inhibiting platinum(IV) prodrugs with potent anticancer activity, Pharmaceutics 14 (2022) 787, https://doi.org/10.3390/pharmaceutics14040787.
[31] Q.Q. Cheng, H.D. Shi, H.X. Wang, Y.Z. Min, J. Wang, Y.Z. Liu, The ligation of aspirin to cisplatin demonstrates significant synergistic effects on tumor cells, Chem. Commun. 50 (2014) 7427–7430, https://doi.org/10.1039/C4CC00419A.
[32] R.K. Pathak, S. Marrache, J.H. Choi, T.B. Berding, S. Dhar, The prodrug platin-A: simultaneous release of cisplatin and aspirin, Angew. Chem., Int. Ed. 53 (2014) 1963–1967, https://doi.org/10.1002/anie.201308899.
[33] B. Surnar, N. Kolishetti, U. Basu, A. Ahmad, E. Goka, B. Marples, D. Kolb, M. E. Lippman, S. Dhar, Reduction of cisplatin-induced ototoxicity without compromising its antitumor activity, Biochemistry-Us 57 (2018) 6500–6513, https://doi.org/10.1021/acs.biochem.8b00712.
[34] J.P. Li, J.M. Guo, E.X. Shang, Z.H. Zhu, Y. Liu, B.C. Zhao, J. Zhao, Z.S. Tang, J. A. Duan, Quantitative determination of five metabolites of aspirin by UHPLC-MS/MS coupled with enzymatic reaction and its application to evaluate the effects of aspirin dosage on the metabolic profile, J. Pharm. Biomed. Anal. 138 (2017) 109–117, https://doi.org/10.1016/j.jpba.2016.12.038.
[35] M.J. Gómez-Lechón, X. Ponsoda, E. O'Connor, T. Donato, J.V. Castell, R. Jover, Diclofenac induces apoptosis in hepatocytes by alteration of mitochondrial function and generation of ROS, Biochem. Pharmacol. 66 (2003) 2155–2167, https://doi.org/10.1016/j.bcp.2003.08.003.
[36] E. Gottfried, S.A. Lang, K. Renner, A. Bosserhoff, W. Gronwald, M. Rehli, S. Einhell, I. Gedig, K. Singer, A. Seilbeck, A. Mackensen, O. Grauer, P. Hau, K. Dettmer, R. Andreesen, P.J. Oefner, M. Kreutz, New aspects of an old drug - diclofenac targets MYC and glucose metabolism in tumor cells, PLoS One 8 (2013), e66987, https://doi.org/10.1371/journal.pone.0066987.
[37] A.P. Duval, L. Troquier, O.D. Silva, N. Demartines, O. Dormond, Diclofenac potentiates sorafenib-based treatments of hepatocellular carcinoma by enhancing oxidative stress, Cancers 11 (2019) 1453, https://doi.org/10.3390/cancers11101453.
[38] L.H. Yang, J.C. Li, Y.Z. Li, Y.L. Zhou, Z.Q. Wang, D.H. Zhang, J.L. Liu, X.D. Zhang, Diclofenac impairs the proliferation and glucose metabolism of triple-negative breast cancer cells by targeting the c-Myc pathway, Exp. Ther. Med. 21 (2021) 584, https://doi.org/10.3892/etm.2021.10016.
[39] A. Galisteo, F. Jannus, A. García-García, H. Aheget, S. Rojas, J.A. Lupiañez, A. Rodríguez-Diéguez, F.J. Reyes-Zurita, J.F.Q. del Moral, Diclofenac N-derivatives as therapeutic agents with anti-inflammatory and anti-cancer effect, Int. J. Mol. Sci. 22 (2021) 5067, https://doi.org/10.3390/ijms22105067.
[40] M. Dooley, C.M. Spencer, C.J. Dunn, Aceclofenac - a reappraisal of its use in the management of pain and rheumatic disease, Drugs 61 (2001) 1351–1378, https://doi.org/10.2165/00003495-200161090-00012.
[41] E. Legrand, Aceclofenac in the management of inflammatory pain, Expet Opin. Pharmacother. 5 (2004) 1347–1357, https://doi.org/10.1517/14656566.5.6.1347.
[42] A.D. Aputen, M.G. Elias, J. Gibert, J.A. Sakoff, C.P. Gordon, K.F. Scott, J.R. Aldrich-Wright, Versatile platinum(IV) prodrugs of naproxen and acemetacin as chemo-anti-inflammatory agents, Cancers 15 (2023) 2460, https://doi.org/10.3390/cancers15092460.
[43] M. Ravera, E. Gabano, S. Tinello, I. Zanellato, D. Osella, May glutamine addiction drive the delivery of antitumor cisplatin-based Pt(IV) prodrugs? J. Inorg. Biochem. 167 (2017) 27–35, https://doi.org/10.1016/j.jinorgbio.2016.11.024.
[44] E. Petruzzella, J.P. Braude, J.R. Aldrich-Wright, V. Gandin, D. Gibson, A quadruple-action platinum(IV) prodrugs with anticancer activity against KRAS mutated cancer cell lines, Angew Chem Int Engl 56 (2017) 11539–11544, https://doi.org/10.1002/anie.201706739.
[45] L. Ma, N. Wang, R. Ma, C. Li, Z. Xu, M.K. Tse, G. Zhu, Monochalcoplatin: an actively transported, quickly reducible, and highly potent Pt(IV) anticancer prodrug, Angew Chem. Int. Ed. Engl. 57 (2018) 9098–9102, https://doi.org/10.1002/anie.201804314.
[46] X. Liu, M.C. Barth, K. Cseh, C.R. Kowol, M.A. Jakupec, B.K. Keppler, D. Gibson, W. Weigand, Oxoplatin-based Pt(IV) lipoate complexes and their biological activity, Chem. Biodivers. 19 (2022), e202200695, https://doi.org/10.1002/cbdv.202200695.
[47] X. Liu, D. Wenisch, M.C. Barth, K. Cseh, C.R. Kowol, M.A. Jakupec, D. Gibson, B. K. Keppler, W. Weigand, Novel oxaliplatin(IV) complexes conjugated with ligands bearing pendant 1,2-dithiolane/1,2-diselenolane/cyclopentyl motifs, Dalton Trans. 51 (2022) 16824–16835, https://doi.org/10.1039/D2DT02217F.
[48] S. Göschl, H.P. Varbanov, S. Theiner, M.A. Jakupec, M. Galanski, B.K. Keppler, The role of the equatorial ligands for the redox behavior, mode of cellular accumulation and cytotoxicity of platinum(IV) prodrugs, J. Inorg. Biochem. 160 (2016) 264–274, https://doi.org/10.1016/j.jinorgbio.2016.03.005.
[49] Y.Y. Scaffidi-Domianello, A.A. Legin, M.A. Jakupec, A. Roller, V.Y. Kukushkin, M. Galanski, B.K. Keppler, Novel oximato-bridged platinum(II) di- and trimer(s): synthetic, structural, and in vitro anticancer activity studies, Inorg. Chem. 51 (2012) 7153–7163, https://doi.org/10.1021/ic300148e.
[50] G.M. Sheldrick, SHELXT - integrated space-group and crystal-structure determination, Acta Crystallogr. A 71 (2015) 3–8, https://doi.org/10.1107/S2053273314026370.
[51] G.M. Sheldrick, Crystal structure refinement with SHELXL, Acta Crystallogr. C 71 (2015) 3–8, https://doi.org/10.1107/S2053229614024218.
[52] O.V. Dolomanov, L.J. Bourhis, R.J. Gildea, J.A.K. Howard, H. Puschmann, OLEX2: a complete structure solution, refinement and analysis program, J. Appl. Crystallogr. 42 (2009) 339–341, https://doi.org/10.1107/S0021889808042726.
[53] Bruker AXS, Apex3 and SADABS, Bruker AXS Inc., Madison, Wisconsin, USA, 2001.
[54] M.S. Novak, G.E. Büchel, B.K. Keppler, M.A. Jakupec, Biological properties of novel ruthenium- and osmium-nitrosyl complexes with azole heterocycles, J. Biol. Inorg. Chem. 21 (2016) 347–356, https://doi.org/10.1007/s00775-016-1345-z.
[55] C. Kretzer, B. Shkodra, P. Klemm, P.M. Jordan, D. Schröder, G. Cinar, A. Vollrath, S. Schubert, I. Nischang, S. Hoeppener, S. Stumpf, E. Banoglu, F. Gladigau, R. Bilancia, A. Rossi, C. Eggeling, U. Neugebauer, U.S. Schubert, O. Werz, Ethoxy acetalated dextran-based nanocarriers accomplish efficient inhibition of leukotriene formation by a novel FLAP antagonist in human leukocytes and blood, Cell. Mol. Life Sci. 79 (2022) 40, https://doi.org/10.1007/s00018-021-04039-7.
[56] M. Werner, P.M. Jordan, E. Romp, A. Czapka, Z.G. Rao, C. Kretzer, A. Koeberle, U. Garscha, S. Pace, H.E. Claesson, C.N. Serhan, O. Werz, J. Gerstmeier, Targeting biosynthetic networks of the proinflammatory and proresolving lipid metabolome, Faseb. J. 33 (2019) 6140–6153, https://doi.org/10.1096/fj.201802509R.